



The Physiological Response of Contrasting Coccolithophore Species to Ocean Alkalinity Enhancement

Sophie Gill^{1,2}, Jiayou Ge^{3,4}, Qiong Zhang^{3,4} , Gideon M. Henderson², and Rosalind E. M. Rickaby² 

¹ISOMETRIC, London, UK, ²Department of Earth Sciences, University of Oxford, Oxford, UK, ³Department of Ocean Science and Centre for Ocean Research in Hong Kong and Macau (CORE), The Hong Kong University of Science and Technology, Hong Kong, China, ⁴Southern Marine Science and Engineering Guangdong Laboratory (Zhuhai), Zhuhai, China

Key Points:

- Increased alkalinity significantly boosts growth rates of coccolithophores *Gephyrocapsa huxleyi* and *Coccolithus braarudii*
- Divergent responses between species arise as large *C. braarudii* rely on CO₂ for calcification, while smaller *G. huxleyi* can use HCO₃⁻ when CO₂ is limited
- Our study suggests constraints for safe ecosystem boundaries (alkalinity << 3,000 μmol kg⁻¹) and offers insights into carbonate chemistry impacts

Supporting Information:

Supporting Information may be found in the online version of this article.

Correspondence to:

Q. Zhang,
qiongz@ust.hk

Citation:

Gill, S., Ge, J., Zhang, Q., Henderson, G. M., & Rickaby, R. E. M. (2025). The physiological response of contrasting coccolithophore species to Ocean Alkalinity Enhancement. *Journal of Geophysical Research: Biogeosciences*, 130, e2025JG009103. <https://doi.org/10.1029/2025JG009103>

Received 16 MAY 2025

Accepted 30 OCT 2025

Author Contributions:

Conceptualization: Sophie Gill, Rosalind E. M. Rickaby

Formal analysis: Sophie Gill, Jiayou Ge, Qiong Zhang

Funding acquisition: Sophie Gill, Qiong Zhang, Rosalind E. M. Rickaby

Methodology: Sophie Gill, Rosalind E. M. Rickaby

Resources: Gideon M. Henderson, Rosalind E. M. Rickaby

Supervision: Qiong Zhang, Gideon M. Henderson, Rosalind E. M. Rickaby

Visualization: Sophie Gill, Jiayou Ge, Qiong Zhang

Abstract Environmental impacts related to the Ocean Alkalinity Enhancement (OAE) on marine biota remain underexplored. Ocean Alkalinity Enhancement aims to increase the ocean's total alkalinity (TA), shifting the carbonate buffer system to prompt air-sea gas exchange and CO₂ drawdown. These conditions might be favorable for calcifiers, leading to increased removal of alkalinity in CaCO₃ and reversing some of the intended benefit of the OAE. Here, we parameterize the impact of increased ocean alkalinity on two dominant end-member coccolithophore species: *Gephyrocapsa huxleyi* and *Coccolithus braarudii*. The growth rate of each species increased significantly with increased alkalinity, likely driven by increasing resupply rates of CO₂ from higher HCO₃⁻ concentrations. Both species increased growth rates relative to the control even at the lowest alkalinity treatments (~3,000 μmol kg⁻¹), which could lead to population expansion under air-equilibrated OAE, and higher population levels of calcification. At higher TA (i.e., >3,000 μmol kg⁻¹), rates of calcification were increasingly limited by CO₂ supply to the faster growing cells which resulted in malformation suggestive that cell division is prioritized over calcification when CO₂-limited. Divergent species-specific responses may arise because large and heavily calcified *C. braarudii* have a far greater carbon demand, and rely on CO₂ for calcification compared to the smaller, lightly calcified rapidly-growing *G. huxleyi* which have the additional capacity to use HCO₃⁻ when CO₂-limited. Our study suggests constraints to ensure safe ecosystem boundaries (i.e., alkalinity 3,000 μmol kg⁻¹), and provides mechanistic insights to understand the impacts of carbonate chemistry on physiology and calcite production by major calcifiers.

Plain Language Summary The marine Carbon Dioxide Removal industry is expanding rapidly, highlighting the need for a better understanding of its environmental impacts. One underexplored area is the effect of Ocean Alkalinity Enhancement (OAE) on marine calcifiers. This study investigates the effects of OAE on two coccolithophore species, *Gephyrocapsa huxleyi* and *Coccolithus braarudii*, which play significant roles in carbon cycling. Our findings indicate that the rate of CO₂ supply, correlated with bicarbonate concentration, is the primary factor influencing growth and calcification rates in both species. Notably, the larger, heavily calcified *C. braarudii* had a higher carbon demand than the smaller *G. huxleyi*, which could explain their differing responses to OAE treatments. Both species growth faster with increasing total alkalinity, suggesting they could thrive under air-equilibrated OAE conditions. However, higher total alkalinity levels constrained calcification rates for faster-growing cells, leading to malformations. While our experimental conditions exceed typical field trial parameters, this study provides important insights into safe operational boundaries and the likely impacts on major calcifying organisms in marine ecosystems.

1. Introduction

Reducing emissions will not be sufficient to meet targets to keep global warming within 2°C (GESAMP, 2019; Gore et al., 2019; Oschlies et al., 2023; Renforth & Henderson, 2017); additional efforts to actively remove carbon dioxide (CO₂) from the atmosphere using Carbon Dioxide Removal (CDR) technologies are needed to achieve the goal (Fuss et al., 2014; Gagern et al., 2022; IPCC, 2001). Ocean Alkalinity Enhancement (OAE) is one of the promising marine CDR pathways that can generate alkalinity directly in seawater through the addition of alkalinity-enhancing materials (Bach et al., 2019; Gagern et al., 2022; Hartmann et al., 2013; Kheshgi, 1995; Oschlies et al., 2023). It has been estimated that through OAE, if the alkalinity of the global surface ocean were raised by an additional 100 to >2,000 μmol kg⁻¹ by the year 2100, this would result in a potential drawdown of 225–5,550 Gt CO₂ (Bach et al., 2019; Feng et al., 2017; Ilyina et al., 2013; Köhler et al., 2010, 2013; Taylor et al., 2017). The CDR industry is growing rapidly, with an estimation of market growth from \$370.0 million in

© 2025. The Author(s).

This is an open access article under the terms of the [Creative Commons Attribution License](https://creativecommons.org/licenses/by/4.0/), which permits use, distribution and reproduction in any medium, provided the original work is properly cited.

Writing – original draft: Sophie Gill,
Qiong Zhang

Writing – review & editing: Sophie Gill,
Jiayou Ge, Qiong Zhang, Gideon
M. Henderson, Rosalind E. M. Rickaby

2022 to \$8.1 billion in 2028 by BCC Research LLC, and marine Carbon Dioxide Removal deployments are planned to occur in the next 5 years. In practice, it is unlikely that significant local perturbations will be pursued in the next 5 years during commercial deployments, due to environmental permitting limits, public acceptance, and an appreciation that minimizing carbonate system perturbations is sensible at this nascent stage of the industry (Isometric, 2024).

OAE raises ocean pH and carbonate saturation state (ΩCaCO_3) to higher values (Ilyina et al., 2013), and therefore it could also contribute to the reversal of ocean acidification, which would have positive co-benefits for many marine organisms at risk due to the inherent rising acidity from equilibration of the increased atmospheric burden of CO_2 with the ocean (Albright et al., 2016; Bach et al., 2019; Doney et al., 2009; Silverman et al., 2007).

Despite being a promising tool for CO_2 drawdown and mitigation of global warming, OAE results in shifting of the surface ocean carbonate buffer system, especially during an initial addition of alkalinity, prior to air-sea equilibration (Bach, 2024; Bach et al., 2019, 2023). At this stage, depending on the concentration of alkalinity added, OAE may cause extreme carbonate chemistry perturbations due to a lower rate of air-sea gas exchange compared to the rapid increase of alkalinity in solution, leading to “hotspots” of alkalinity addition with severely decreased $p\text{CO}_2$ in addition to increased pH and ΩCaCO_3 (Bach et al., 2019; Ilyina et al., 2013). Hartmann et al. (2023) found that an application of reactive alkaline solids $\sim 600 \mu\text{mol kg}^{-1}$ above control conditions for some hydroxide treatments reduced OAE efficiency (i.e., net loss in alkalinity), although the authors noted that more research is needed to establish sustainable application boundary conditions and management procedures for OAE.

While there is a growing body of research on OAE, some unknown impacts of OAE in the marine environment, particularly on marine biota, have not yet been assessed extensively in laboratory (Faucher et al., 2025; Iglesias-Rodríguez et al., 2023) or field experiments (Bednaršek et al., 2024; Dupont & Metian, 2023; Oschlies et al., 2023). Calcifiers may be one of the most sensitive organisms to proposed OAE schemes because they are the most sensitive organisms to carbonate system perturbations induced by ocean acidification (Gattuso et al., 2018). The lowered H^+ and elevated saturation state associated with OAE could promote calcification (Bach et al., 2015; Cyronak et al., 2016; Monteiro et al., 2016). Coccolithophores are one of the three major groups of calcifying plankton in the modern oceans, alongside foraminifera and pteropods (Monteiro et al., 2016; Sarmiento & Gruber, 2013). They are also estimated to be responsible for up to 10% of global organic carbon fixation (O'Brien et al., 2016; Perrin et al., 2016; Poulton et al., 2007). Previous studies mostly focused on the impacts of ocean acidification on coccolithophores (Beaufort et al., 2011; Iglesias-Rodríguez et al., 2008; Kottmeier et al., 2016; Richier et al., 2011; Xu et al., 2023). Documentation of the effects of OAE on different coccolithophores are still limited, while manipulations of total alkalinity (TA) were found to have insignificant impact on the growth and calcification of the species *Emiliana huxleyi* (Faucher et al., 2025; Gately et al., 2023). More studies are needed to understand how different coccolithophore species respond uniquely to OAE, both in culture and in natural settings (Chauhan et al., 2024; Subhas et al., 2022).

Gephyrocapsa huxleyi (previously known as *Emiliana huxleyi*, Bendif et al., 2019), a small coccolithophore from the family *Noelaerhabdaceae*, genus *Reticulofenestra* (Stevenson et al., 2014), is by far the main bloom-forming coccolithophore (Tyrrell & Merico, 2004), and is the model organism for most coccolithophore studies due to its ubiquitous presence in our surface oceans (Blanco-Ameijeiras et al., 2016; Mayers et al., 2016). *G. huxleyi* is a significant contributor to global coccolithophore biomass, accounting for more than half of the organic standing stocks of coccolithophore worldwide (de Vries et al., 2021). *Coccolithus braarudii* is a much larger coccolithophore and evolved from the *Coccolithus* genus. Despite being much less abundant in the modern surface ocean, *C. braarudii* produces a comparable amount of calcite to *G. huxleyi* globally (Poulton et al., 2007) and in some communities/regions may produce more than *G. huxleyi*, for example, the Arctic Ocean (Daniels et al., 2014). These two contrasting genera of coccolithophores are often used as “endmembers” in previously published studies (Hermoso et al., 2014; Rickaby et al., 2010; Walker et al., 2018). This is because (a) the physiologies of these small and large coccolithophore genera have been inferred to differ in their control of internal pH and modes of carbon acquisition (Chauhan & Rickaby, 2024; Rickaby et al., 2010), (b) the cellular calcite content of *C. braarudii* is often 30–80 times higher than that of *G. huxleyi* (Daniels et al., 2014), and (c) *G. huxleyi* generally grows faster than *C. braarudii* even under identical conditions (Daniels et al., 2014). Additionally, the differing responses of *G. huxleyi* and *C. braarudii* to ocean acidification highlight the importance of

examining the potential of these two species and the genera from which they originate to differ in their response to significant shifts in carbonate chemistry, such as those might occur during OAE (Meyer & Riebesell, 2015).

Recently, isotopic vital effects, of coccolith calcite grown at different CO_2 have revealed the contrasting carbon species dominating the supply for calcification by *C. braarudii* compared to the *Gephyrocapsids*, including *G. huxleyi* (Chauhan & Rickaby, 2024). It has long been assumed that seawater HCO_3^- is the major source of carbon for calcification, based on the close correlation of stable C isotopes in coccolith calcite with the HCO_3^- of seawater (Buitenhuis et al., 1999; Sikes et al., 1980). In practice, it is hard to distinguish between these mechanisms based on the isotopic correlation with seawater HCO_3^- , because it is difficult to distinguish isotopic signals of directly imported HCO_3^- , from CO_2 that diffuses and then re-speciates via internal hydration to intracellular HCO_3^- .

A multi-species experiment across a wide range of CO_2 availabilities revealed the characteristic signature of a diffusive supply of CO_2 as a source of carbon to the internal site of calcification in the Coccolithales. The tendency of the C isotopic signal toward -10‰ during extreme CO_2 limited growth of *C. Leptoporus*, and *C. braarudii*, both large, slow growing heavily calcifying species points to the quantitative transformation of isotopically unequilibrated carbon dioxide into calcite inside the cells. This is suggestive that these large, carbon-demanding species are characterized by a highly depleted internal pool, and points to diffusive CO_2 being the only carbon source, so providing a definitive fingerprint of this carbon species dominating the carbon supply for the internal calcification (Chauhan & Rickaby, 2024).

By contrast, for the small, fast growing Gephyrocapsid species grown under varying CO_2 availability, the coccoliths display a covariation of C and O isotopes, with a gradient close to the mass-dependent fractionation slope of 0.5. During carbon limited growth, these species generate liths with isotopes that are heavier in both C and O isotopes- at the other extreme of the isotopic gradient than the light isotopes of the CO_2 limited growth of *C. leptoporus* and *C. braarudii*. Such a gradient in the small, faster growing cells, and isotopically heavy composition, points to a kinetic isotopic fractionation, underlying the isotopic vital effect associated with the diffusion of isotopically light CO_2 out of the cells when grown under low CO_2 conditions. At low CO_2 availability, the cells are able to concentrate carbon at levels inside the cell to levels higher than those outside of the cell. But the buffering of carbon is poor due to the low residence time of Ca and C in the small internal pool (Branson et al., 2025), such that there is an outwards CO_2 diffusive flux and loss of isotopically light CO_2 from the site of calcification. Such observations align with the MIMS experiments run by Rost & Riebesell., 2004, showing the outwards diffusion of CO_2 from *G. huxleyi* when the light is switched off, and also develops further the concept that these species upregulate HCO_3^- at low CO_2 (Bach et al., 2013; Kottmeier et al., 2014, 2016). The Gephyrocapsids use a co-transport mechanism facilitated by proteins belonging to the SLC4 family of bicarbonate transporters (Mackinder et al., 2011) and so have an additional capacity for HCO_3^- uptake to supplement diffusive CO_2 supply when it is less available, a pathway which may be absent in the Coccolithales (Accession number: PRJNA1321905).

Given the representativeness of these species, with contrasting size, growth rate and calcification intensity, for the two dominant, anciently divergent groups of modern coccolithophores, and their contrasting carbonate chemistry dependence, our data can provide insights into the likely responses of the majority of coccolithophores in the contemporary ocean. Here we examined the growth, calcification response, and morphology of these two key “endmember” species of coccolithophore (*G. huxleyi* and *C. braarudii*) to OAE using in vitro laboratory culture experiments. We also compared how the addition of the monovalent cation Na^+ and divalent cation Ca^{2+} to raise TA affected growth and calcification responses.

2. Materials and Methods

2.1. Simulation of Air-Equilibrated OAE

Two different pathways to simulate OAE were used: (a) adding NaHCO_3 to Synthetic Ocean Water (SOW), and (b) adding $\text{Na}_2\text{CO}_3 + \text{CaCl}_2$ to SOW. These pathways compare the effect of alkalinity added as Na^+ versus Ca^{2+} . Since calcium bicarbonate, $\text{Ca}(\text{HCO}_3)_2$, does not exist in solid-state, $\text{Na}_2\text{CO}_3 + \text{CaCl}_2$ were applied to simulate $\text{Ca}(\text{HCO}_3)_2$ addition to SOW to make it comparable to the SOW + NaHCO_3 pathway. In both pathways, the TA was set from control SOW values representing natural seawater condition ($\sim 2,500 \mu\text{mol kg}^{-1}$) up to $\sim 1,500 \mu\text{mol kg}^{-1}$ above the control as the most extreme OAE scenario ($\sim 4,000 \mu\text{mol kg}^{-1}$, Table S1 in

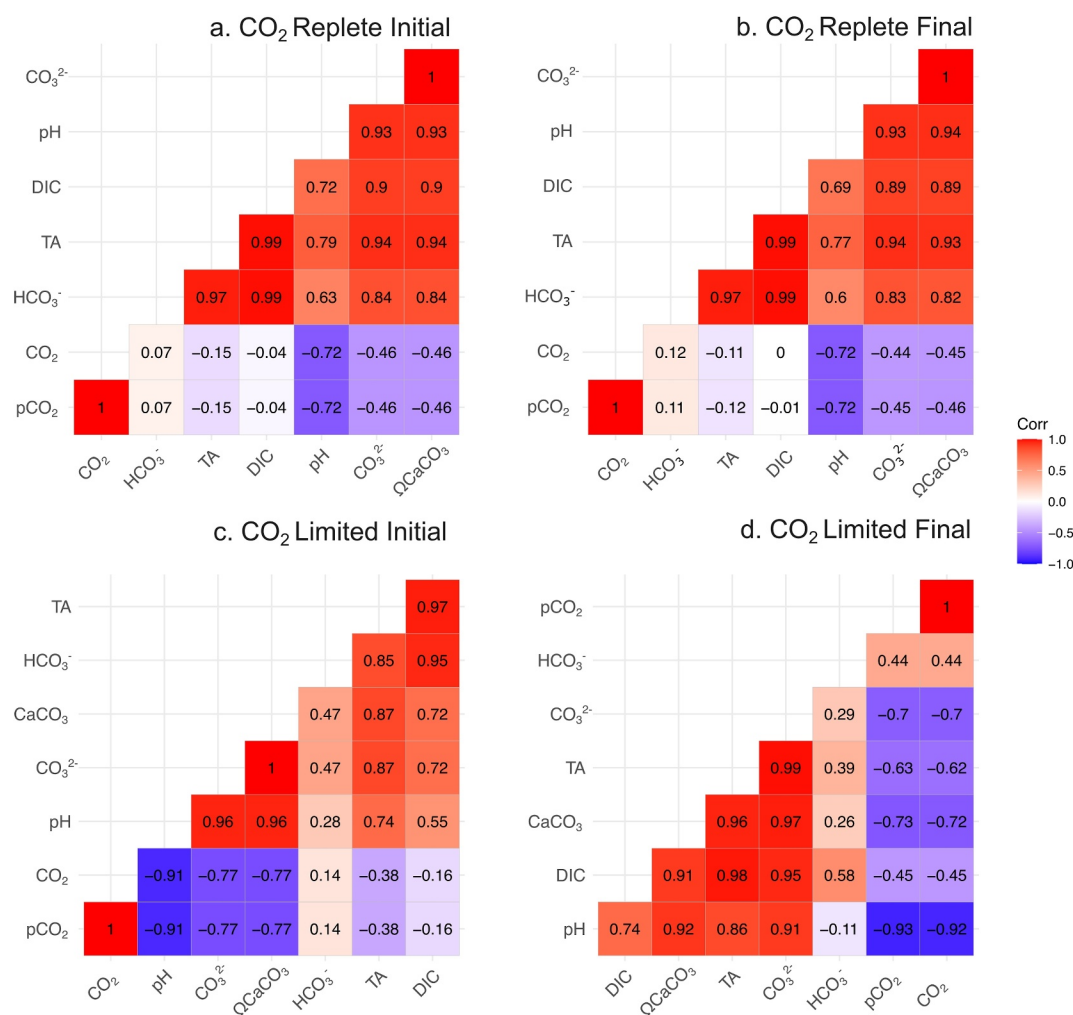


Figure 1. Correlation analysis on carbonate chemistry parameters in growth media before (a, c) and after (b, d) the culture experiments under CO₂-replete (low cell density, a, b) and CO₂-limited (high cell density, c, d) conditions.

Supporting Information S1). Solutions were then bubbled with ambient air for 120 min to equilibrate the seawater carbonate system with atmospheric CO₂. In both pathways, [CO₂] did not change after 120 min and the solutions were therefore inferred to have achieved equilibration with the atmosphere in that time (Figure S1 in Supporting Information S1). Before inoculating the experimental cultures, the media was 0.22 μm filter-sterilized and sealed in parafilm 2 L polycarbonate bottles. Samples for initial TA for the culture media were taken from this 0.22 μm filter-sterilized culture media, parafilm to prevent any evaporation which would affect alkalinity levels and stored at 4°C before analysis. The starting carbonate chemistry of all experimental manipulations relative to increasing TA is shown in Figures S2 and S3 in Supporting Information S1 and Table S1 in Supporting Information S1, and the correlations of different carbonate system parameters are shown in Figure 1.

2.2. CO₂-Replete Versus CO₂-Limited Cultures

Coccolithophore *G. huxleyi* strains RCC911 and SO 14-2, and *C. braarudii* strain RCC1198 were cultured in incubators at a constant temperature of 16 ± 1°C and illuminated with 100 ± 5 μmol photons m⁻² s⁻¹ on a day-to-night cycle of 14:10 hr in all experiments. For the two *G. huxleyi* strains, RCC 911 is in genetic subgroup A2, and SO14-2 (OA15) in A1d (Bendif et al., 2023), but morphologically they are very similar in cell size and calcification intensity; these cellular traits may be more important than genetic differences in dictating response to ocean chemistry.

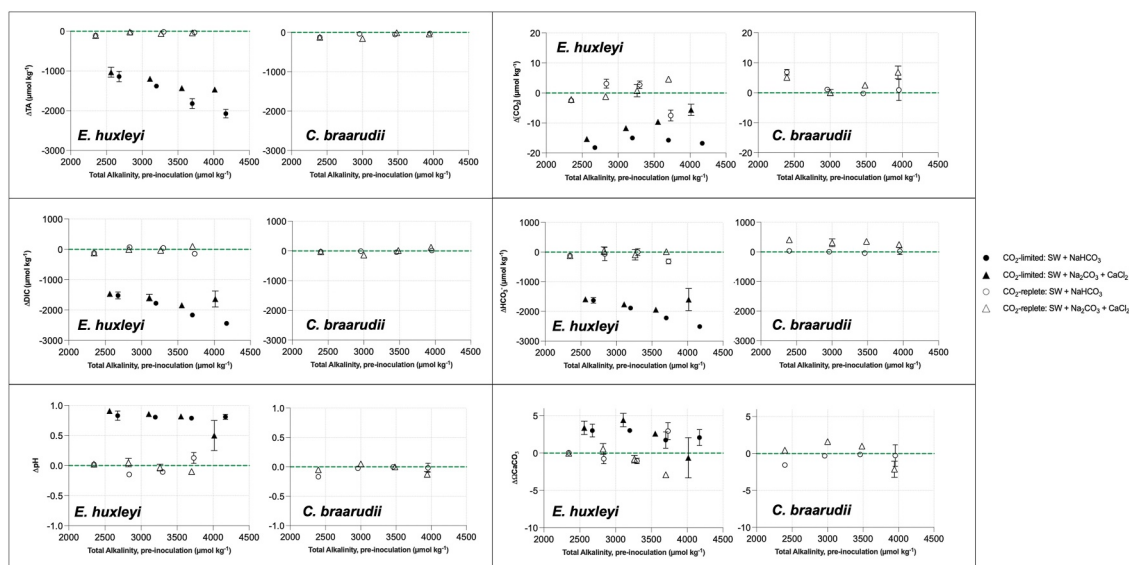


Figure 2. Drifts in carbonate system parameters in CO₂-replete and CO₂-limited cultures (legend on right-hand side) between pre-inoculation and cell harvest.

In our experiments, culture medium was prepared using SOW with different levels of TA, and enriched with 882 $\mu\text{mol L}^{-1}$ nitrate, 36.2 $\mu\text{mol L}^{-1}$ (37.286 $\mu\text{mol kg SW}^{-1}$) phosphate, and 106 $\mu\text{mol L}^{-1}$ silicate (109.18 $\mu\text{mol kg SW}^{-1}$), with trace metals and vitamins according to the L1 medium recipe (Guillard & Hargraves, 1993).

Before inoculation of the experiments, all cultures were pre-acclimated to the control or enhanced alkalinity conditions in small-volume, dilute cultures for a minimum of 5 generations, to ensure that growth and calcification responses measured in the final experiments were adapted growth responses (Riebesell et al., 2010). These small-volume acclimated cultures were manually agitated during pre-acclimation by daily gentle inversion and subsampled at dilute culture densities in the exponential phase for inoculating the experimental cultures to avoid significant drift in the carbonate system.

CO₂-replete experiments were done with *G. huxleyi* strains RCC911 and *C. braarudii* strain RCC1198 and were carried out following best practices (Riebesell et al., 2010) for dilute culturing ensuring that CO₂(aq) was above 10 $\mu\text{mol/kg}$ throughout the experiment. In these experiments, Dissolved Inorganic Carbon (DIC) drawdown over the course of culturing was <5% (Figure 2, Table S2 in Supporting Information S1), meaning that there was no significant drift in the carbonate chemistry of the media, and so [CO₂] was replete throughout the experimental incubations: these experiments were representative of an air-equilibrated OAE scenario. At the beginning of the CO₂-replete experiments, ~ 100 cells mL⁻¹ of *G. huxleyi* (Riebesell et al., 2010) and ~ 400 cells mL⁻¹ of *C. braarudii* (Hermoso, 2015) in each experimental alkalinity treatment were inoculated in 600 mL triplicates, and culture flasks were manually agitated daily. The cultures were harvested after growing for a minimum of five generations in the exponential phase when cell densities reached a maximum of 60,000–100,000 cells mL⁻¹ for *G. huxleyi* (Bach et al., 2013; Riebesell et al., 2010), and 5,000–6,000 cells mL⁻¹ for *C. braarudii* (Hermoso, 2015).

The coccolithophore *G. huxleyi* is known to form algal blooms, during which the cell density could attain more than 10⁷ cells/mL (Harlay et al., 2010; Kubryakov et al., 2019). Such a high cell density could lead to a greater rate of uptake of CO₂, than the rate of replenishment to the surface waters via air-sea exchange which alters the temporal carbonate chemistry and can feed back on cell physiology during OAE. We also inoculated the phytoplankton at much higher cell densities ($\sim 1,000$ cells mL⁻¹, ~ 10 times greater than recommended value (Riebesell et al., 2010)) and then allowed the cultures to grow to very high densities ($2\text{--}3 \times 10^6$ cells mL⁻¹) before the point of harvest at the late exponential phase, to mimic potential blooming conditions (Harlay et al., 2010; Kubryakov et al., 2019). [CO₂] reached <1 $\mu\text{mol kg}^{-1}$ in these experiments by the time of harvest (Table S2 in Supporting Information S1, Figure 2), below *G. huxleyi*'s threshold for CO₂-limitation (Sett et al., 2014) so the cells were severely CO₂-limited at the end of the experimental incubations. To keep

Table 1
Experimental Conditions Used for Different Strains in This Study

Species	CO ₂ -replete (non-blooming)		CO ₂ -limited (blooming)	
	P1 – SOW + NaHCO ₃	P2 – SOW + Na ₂ CO ₃ + CaCl ₂	P1 – SOW + NaHCO ₃	P2 – SOW + Na ₂ CO ₃ + CaCl ₂
<i>Gephyrocapsa huxleyi</i>	✓	✓	✓	✓
<i>Coccolithus braarudii</i>	✓	✓	✗	✗

consistency in alkalinity treatments, CO₂-limited experiments were achieved by using the same alkalinity addition pathways and equilibration methods as in the CO₂-replete experiments. The CO₂-limited experimental incubations were done on *G. huxleyi* only (strain SO 14-2 (morphotype A)).

The strains for CO₂-replete and CO₂-limited *G. huxleyi* experiments are different due to constraints on strain availability before and after the COVID-19 pandemic. Both RCC911 and SO 14-2 are morphotype A. *G. huxleyi* in the same morphotype commonly show similarities in growth, calcification, morphology and share similar genetic material (Cook et al., 2011; Rigual-Hernández et al., 2020). Therefore, the results from both strains can be robustly compared. A summary of the experiments completed on the different strains and conditions is shown in Table 1. Under each condition, at least three replicates were cultured for each strain to account for variation in biological responses to OAE manipulations.

2.3. Growth Rates

Cell count (cells mL⁻¹) and coccosphere size (μm) were measured every day using a Beckman Coulter Counter Z2 analyzer. Specific growth rates were calculated using the following equation during the exponential phase of growth (Figure S8 in Supporting Information S1):

$$\mu = \frac{\ln N_t - \ln N_0}{t}$$

where N_0 represents the initial cell count, N_t represents the current cell density after a time t with a growth rate μ (d⁻¹) (Rickaby et al., 2002; Zondervan et al., 2001).

2.4. Alkalinity Measurement and Carbonate System Calculation

During the experiments, 9 mL alkalinity samples were collected each day by 0.22 μm syringe-filtering the culture medium. Total Alkalinity (TA) of the solutions at each timestamp was measured with an average precision of ~9 μmol kg⁻¹ on duplicate samples by Gran titration using a Metrohm Ti-touch 916. The 9 mL samples were split into 3 mL triplicate samples to analyze on the autotitrator. The autotitrator was calibrated daily against a certified seawater reference material (Dickson Batch 174, Scripps Institute of Oceanography, measured at ~21 μmol kg⁻¹ precision). The pH of each solution was measured using the 867 pH module, which was calibrated daily against standard NBS buffers. Subsequent calculation of the rest of the carbonate system was completed using CO2SYS v2.1 (Pierrot et al., 2011), with inputs of TA and pH, K_1 , and K_2 constants (Roy et al., 1993), KHSO₄ values from Dickson, pH on the NBS scale and [B]_T value (Lee & Morse, 2010) and showed the expected inverse relationship between TA, HCO₃⁻ and for example, CO₂(aq) was preserved across all of our treatments (Figure 1).

2.5. Calcification Rates

Since coccolithophores extract alkalinity from the culture medium as they calcify, we applied the alkalinity anomaly technique for calculating calcification rates in this study (Chisholm & Gattuso, 1991; Cohen et al., 2017). This technique generally assumes that the uptake of nutrients negligibly affects the change of TA (ΔTA) in the medium, and that the processes of respiration and photosynthesis do not affect ΔTA. Chisholm and Gattuso (1991) confirmed that all underlying assumptions of the alkalinity anomaly technique are correct, and no correction for nutrient changes are required in the calculation of calcification because these changes are smaller than the variation in actual calcification values (Chisholm & Gattuso, 1991).

Here, calcification rate (RCa) for the cultures is calculated using the equation below:

$$RCa(\text{pg cell}^{-1}d^{-1}) = \left(\frac{1}{2} \cdot \frac{\Delta TA}{\Delta \text{Cells mL}^{-1}} \right) \cdot d^{-1}$$

Where ΔTA is the change in TA in the final culture medium compared to the initial culture medium.

2.6. Scanning Electronic Microscopic (SEM) Analysis

SEM samples were taken at harvest from the triplicate 600 mL cultures by pipetting 10 mL of culture onto a 47 mm polycarbonate filter (0.6 μm pore size) and filtering gently using a Whatman filter pump. Cells on the filter were alternately washed with 10 mM CaCl_2 solution and 100% Ethanol 3–5 times before drying in a laminar flow hood overnight. Samples were then gold-coated and imaged on a Zeiss Sigma 300 Field Emission Gun Scanning Electron Microscope.

Malformation statistics were generated from a collection of SEM images using a combination of manual observations and ImageJ. For each image of either coccospheres or free liths from each experimental condition, every individual lith was categorized as follows: (a) not malformed if there was no evidence of malformation, (b) mildly malformed if <50% of the total lith was malformed, or (iii) severely malformed if $\geq 50\%$ of the total lith was malformed. Examples of liths that fit into each of these categories for *G. huxleyi* and *C. braarudii* and the total number of liths analyzed for each experimental treatment are included in full in Table S3–S5 in Supporting Information S1.

2.7. Statistical Analysis

Data generated from different alkalinity treatment groups were tested for significant difference using one-way ANOVA and the post-hoc Tukey-Kramer test. Before these statistical analyses, data were tested for normality using the Shapiro-Wilks test (Gore et al., 2019; Shafiee et al., 2021). If data did not pass the test for normality using Shapiro-Wilks, the Kruskal-Wallis test for significant difference and Dunn's multiple comparison test were used following best practice guidelines for statistical analysis.

3. Results

3.1. Growth and Calcification Response to Enhanced TA

Under CO_2 -replete conditions, similar trends of growth and calcification responses were observed from both coccolithophore species investigated in this study, but the degrees of change were different. The growth rates of *G. huxleyi* generally increased with HCO_3^- and TA (Figures 3b and 3c, $p < 0.001$) but decreased with the inversely related carbonate system parameters $[\text{CO}_2]$ under CO_2 -replete conditions (Figure S4a in Supporting Information S1, $p = 0.004$). The change in growth rates in *C. braarudii* was not as significant as in *G. huxleyi* under different TA treatments (Figures 3a–3c) but did record a significant increase in growth rates with increasing CO_3^{2-} ($p < 0.001$) and pH ($p < 0.001$) which both correlate with TA (Figure S4 in Supporting Information S1; Figure 1). However, *C. braarudii* exhibited a much stronger decrease of calcification rates in response to the increase of TA and the other co-varying parameters (Figures 1 and 3d–3f), compared to the less stark decrease in calcification observed in *G. huxleyi* in response to the increase of TA. An increase of calcification rate was observed in *G. huxleyi* with $[\text{CO}_2]_{\text{aq}}$ and $p\text{CO}_2$ ($p < 0.001$), while the correlations of calcification rates of *C. braarudii* with $[\text{CO}_2]$ and $p\text{CO}_2$ were insignificant (Figure S4 in Supporting Information S1, $p > 0.05$). Integrating all data together from all experiments with *G. huxleyi* (CO_2 limited and CO_2 deplete) with the mean $\text{CO}_2(\text{aq})$ of the culture (Faucher et al., 2025), suggests that growth rates and calcification rates increased in proportion to the availability of $\text{CO}_2(\text{aq})$ (Figure 5, $p < 0.0001$).

3.2. Responses of Coccolithophores to the Two Pathways and CO_2

Under CO_2 -replete conditions, for both species investigated in the study, no significant difference in the growth and calcification response was observed between the two pathways employed for increasing TA (Figure 3, Figures S4, S5, S7a, and S7b in Supporting Information S1). However, under CO_2 -limited conditions (high cell density), the growth and calcification responses to the increase of TA and other co-varying parameters were clearly distinguishable in the two pathways (Figure 4, Figures S6 and S7c in Supporting Information S1). Within each pathway, the growth of *G. huxleyi* did not change significantly between different TA treatments, but the

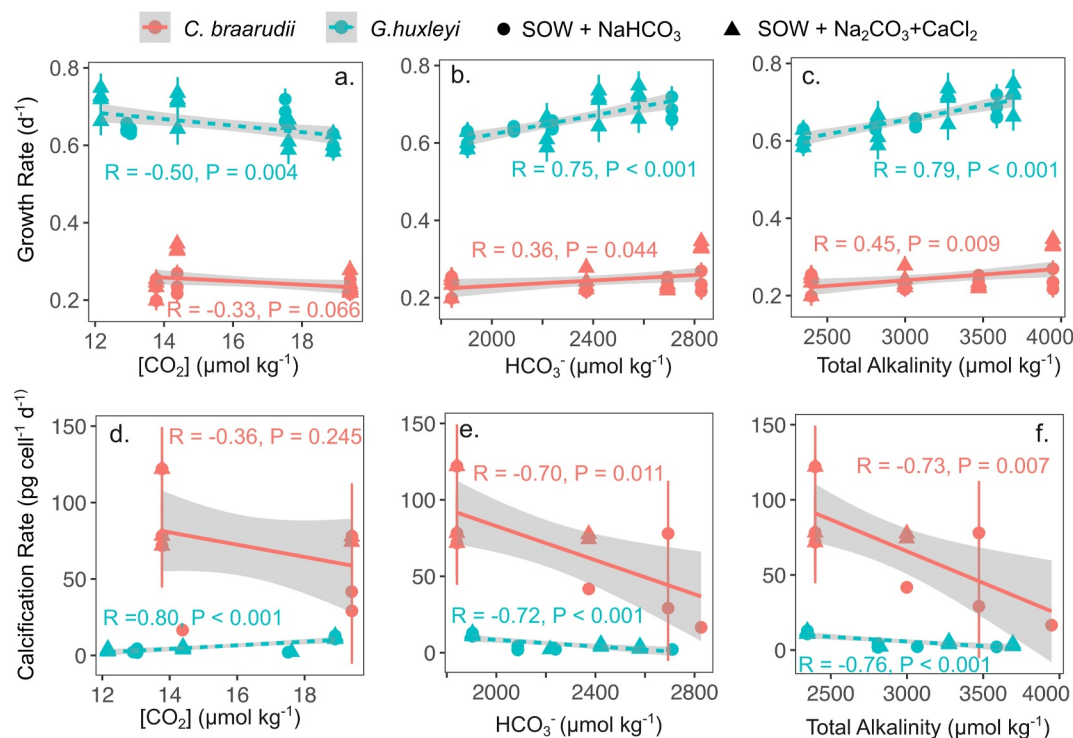


Figure 3. Specific growth (a–c) and calcification rates (d–f) of *C. braarudii* and *G. huxleyi* in response to individual initial carbonate system parameters under CO₂ replete conditions in culture media: (a, d) [CO₂], (b, e) HCO₃⁻, (c, f) Total Alkalinity. Each symbol represents an individual replicate of the culture experiment. Error bars represent the standard deviation of samples from each group ($n = 3$). The lines show the linear fitting of the data, with 95% confidence intervals shown in gray shade. For the linear fittings, $p < 0.05$ indicates that the fitting is statistically significant. The relationships between specific growth and calcification rates of the two species in response to other carbonate system parameters are shown Figures S4 and S5 in Supporting Information S1.

growth rates in Pathway I (Na-pathway) were much higher than those in Pathway II (Ca-pathway). The significant difference in the Na- and the Ca-pathway appears to have arisen by an unintended difference in the initial concentration of [CO₂], which is highly sensitive to small changes in carbonate chemistry, in the pathways (Figure 4a) with a growth rate ($\mu \sim 0.3 \text{ day}^{-1}$) for *G. huxleyi* in the Na-pathway double that of the lower CO₂ Ca-pathway ($\mu \sim 0.15 \text{ day}^{-1}$). Furthermore, the growth rates of the CO₂-limited *G. huxleyi* cells were ~ 3 times lower compared to those at CO₂-replete conditions (Figures 3 and 4) in all alkalinity groups, which highlights the importance of the availability of [CO₂] for the growth rate of this species (Figure 5). In Pathway I, a general increase of growth rates with HCO₃⁻ and TA was observed, but no correlation was found in Pathway II, potentially because the cells were so extremely limited by the availability of CO₂. There are relatively strong positive correlations between cellular calcification rates and both the HCO₃⁻ and TA (Figures 4e and 4f, $p < 0.05$). There is also a reasonably strong trend of decreasing cellular calcification rate with increasing [CO₂], especially in pathway II (the Ca-pathway) (Figure 4d, $p = 0.002$).

3.3. Coccosphere Size and Malformation

There is strong evidence that coccosphere size increased with increasing TA for CO₂-limited cultures of *G. huxleyi*, whereas coccosphere size did not change with increasing TA in CO₂-replete conditions (Figure 6a). As shown in Figure 4f, cellular calcification rate increased with increasing TA under CO₂-limited conditions. In both CO₂-limited and CO₂-replete conditions, *G. huxleyi* showed an increased tendency toward malformed liths with increasing TA (Figures 7a–7d and 8).

As for *C. braarudii*, there were no trends in coccosphere size that were linked to increasing TA. *C. braarudii* cultures showed no particularly clear trends in malformation with increasing TA but were generally more

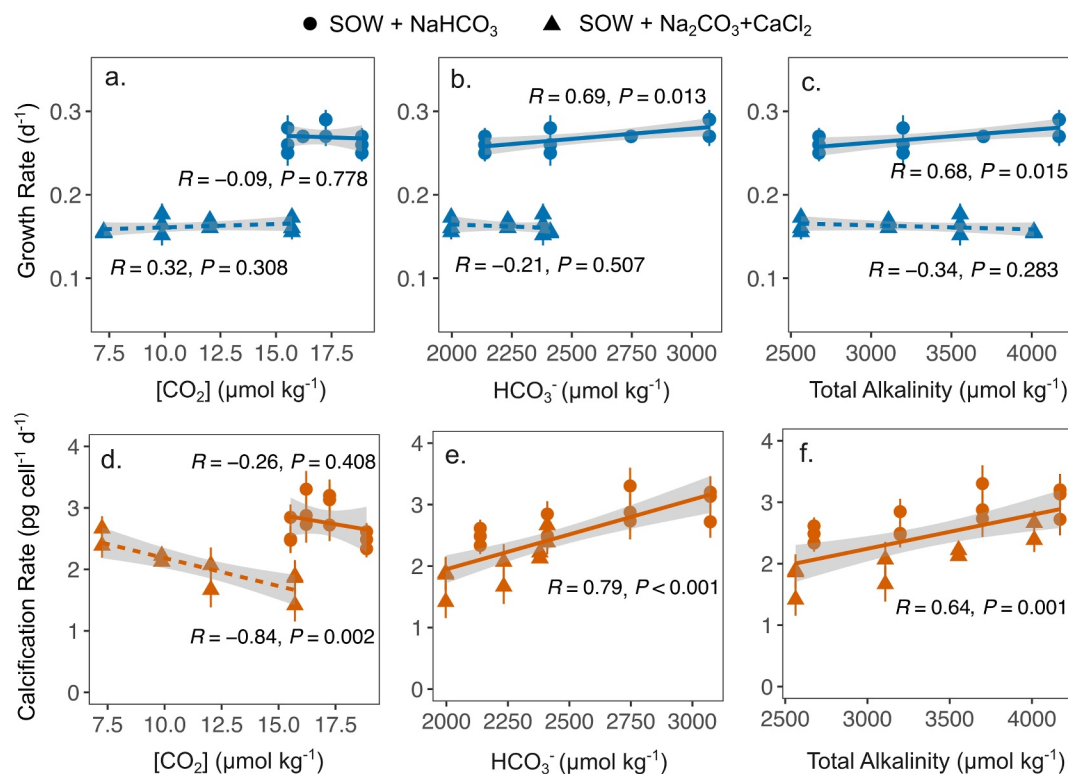


Figure 4. Specific growth rates (a–c) and calcification rates (d–f) of CO₂-limited *G. huxleyi* in response to initial carbonate system parameters in culture media: (a, c) [CO₂], (b, e) HCO₃⁻, (c, f) Total Alkalinity. Each symbol represents an individual replicate of the culture experiment. Error bars represent the standard deviation of samples from each group ($n = 4$). The lines show the linear fitting of the data in each group, with 95% confidence intervals shown in shade. The solid lines represent the linear fitting of the data from the Na pathway, while the dash lines represent those from the Ca pathway, except that for subfigure m, the linear line represents the linear fitting for all data from both pathways. For the linear fittings, $p < 0.05$ indicates that the fitting is statistically significant. The relationships between specific growth and calcification rates of the CO₂-limited *G. huxleyi* in response to other carbonate system parameters are shown Figure S6 in Supporting Information S1.

malformed (most notably severe malformation increased) with increasing TA relative to control conditions (Figures 7e–7f and 8).

4. Discussion

In all our experiments, we maintained consistent light intensity, light-dark cycles, and temperature and the experiments were started with the same nutrient concentrations which are more replete than the typical natural environment. The only variable in the experimental conditions was the carbonate chemistry which allowed a

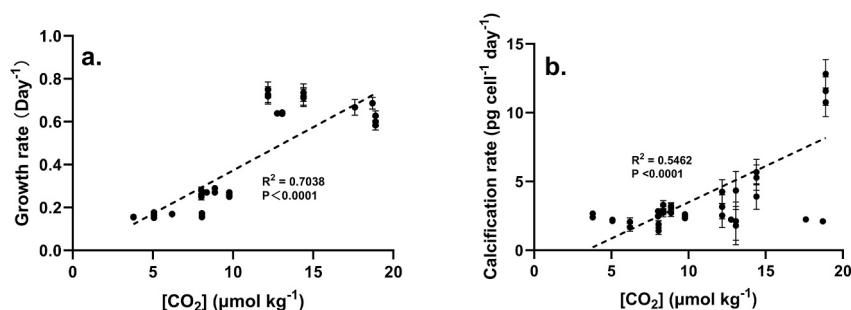


Figure 5. Specific growth (a) and calcification rates (b) of *G. huxleyi* in response to the mean CO₂ concentrations experienced during the culture experiment under different total alkalinity treatment groups. The mean CO₂ concentrations were calculated as the mean of the initial and final CO₂ concentrations in each group.

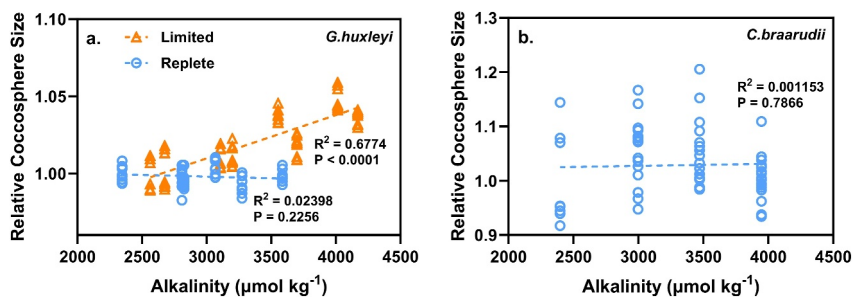


Figure 6. The relative coccosphere size versus total alkalinity set in the experiments in both CO₂-replete and CO₂-limited conditions in *G. huxleyi* (a) and that in CO₂-replete conditions in *C. braarudii* (b). Each symbol represents an individual sample measurement. The lines show the linear fitting of the data in each group, with 95% confidence intervals shown in shade. For the linear fittings, $p < 0.05$ indicates that the fitting is statistically significant.

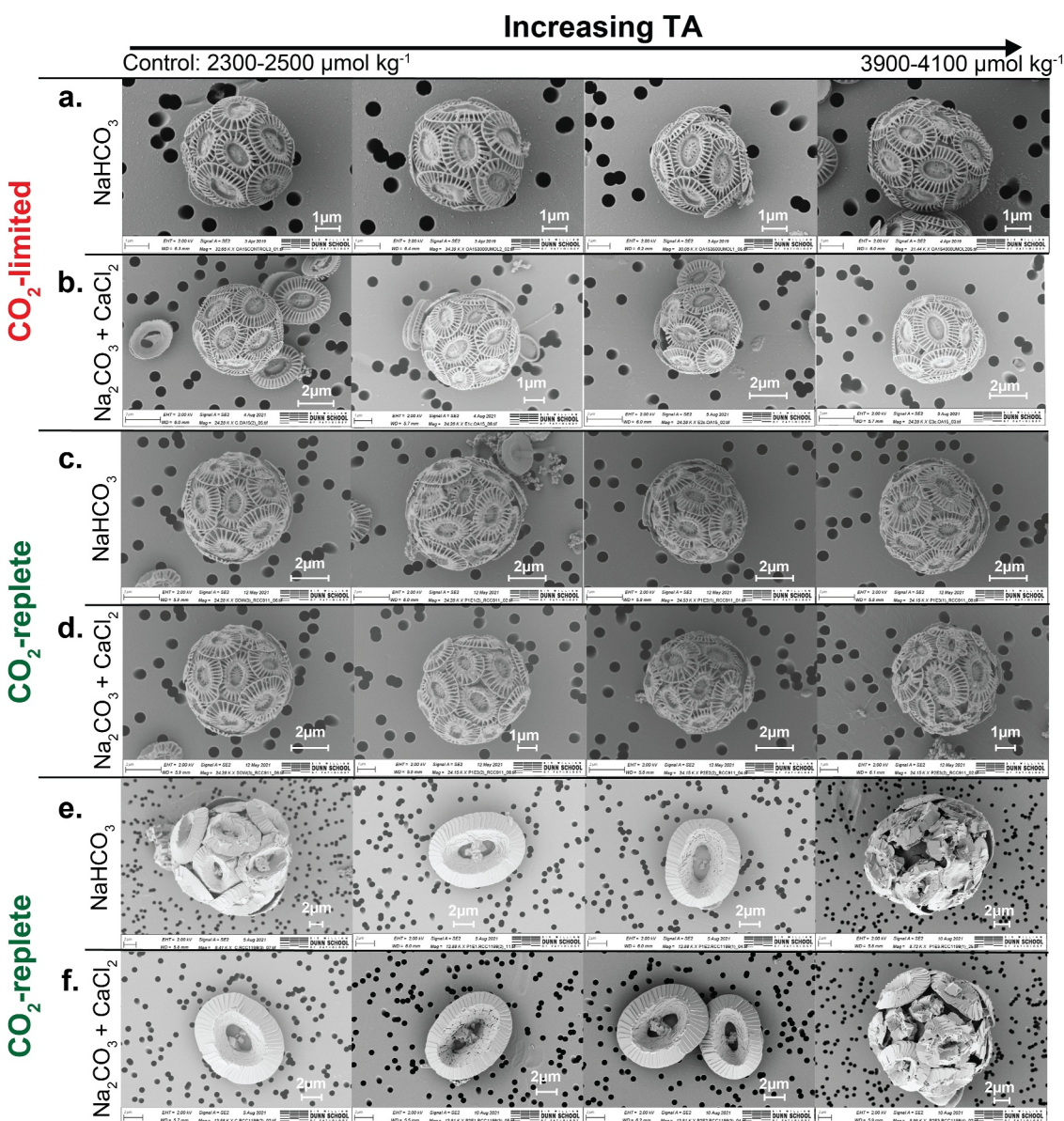


Figure 7. Scanning Electronic Microscopic images taken of *G. huxleyi* (a–d) and *C. braarudii* (e, f) at cell harvest. Trendline shown for increasing total alkalinity.

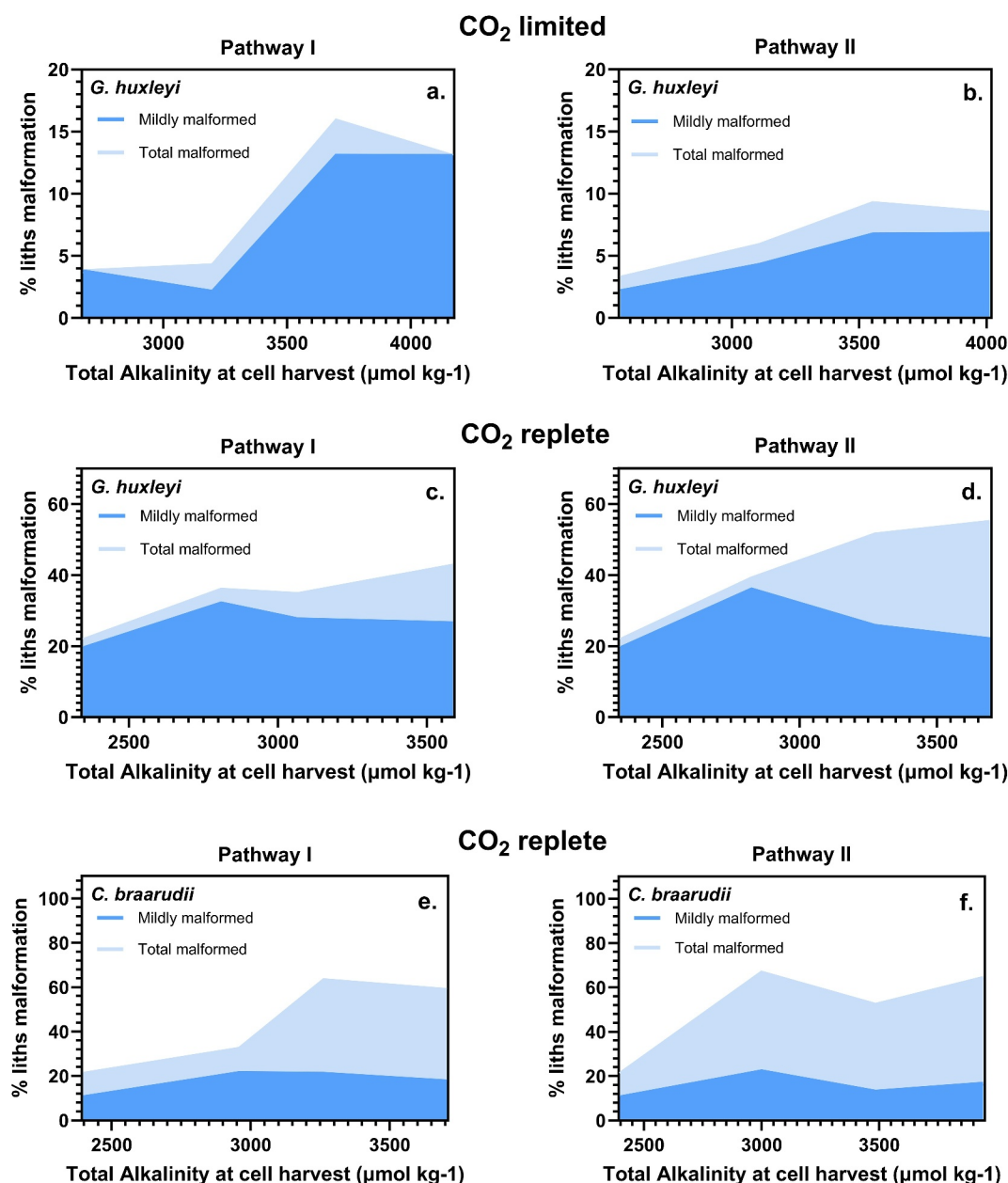


Figure 8. The percentage of malformed liths observe at different total initial alkalinity (total alkalinity) levels set in the experiments. Upper line on each graph = total % of liths malformation observed. Lighter blue area = % of liths exhibiting severe malformation. Darker blue area = % of liths exhibiting mild malformation. Note that for better visualization, the scales for y axes are different. The data for severity levels of malformation are shown in Table S3–S5 in Supporting Information S1.

mechanistic insight into the responses of the different species. Consequently, the variations in physiological responses of the same species among different alkalinity groups were likely driven by changes in seawater carbonate chemistry. Nonetheless, our experiments assessed only short term adapted responses over a few generations, and only investigated single strains. We minimized carbonate chemistry drift in the CO₂-replete cultures (Figure 2), but there was carbonate chemistry drift in the CO₂-deplete experiments as evident in other published studies (Faucher et al., 2025; Gately et al., 2023) due to the inevitable reduction in CO₂(aq) as a consequence of elevated alkalinity. Unlike the natural environment where waters are in constant motion, our cultures may have experienced some degree of boundary layer development around the cells despite regular agitation.

Seawater alkalinity is predominantly composed of bicarbonate (HCO_3^-), carbonate (CO_3^{2-}) and to a much smaller extent hydroxide (OH^-) anions that are charge balanced by cations other than H^+ . The preceding chemical bases then constitute nearly all of seawater's carbonate alkalinity. During OAE, different components of the surface ocean carbonate system will shift their speciation as a result of TA addition to the surface ocean and such change can be directly sensed by marine biota and induce their different physiological responses. Under conditions of rapid growth, such as during a spring bloom, phytoplankton activity might significantly alter temporal seawater carbonate chemistry after TA addition, due to fast CO_2 utilization by cells which could not be equilibrated with sea-air exchange, and such perturbation could further impact phytoplankton responses to varying degrees of TA addition.

4.1. Growth Under OAE

For *G. huxleyi*, from the observations of the biggest range in growth rate being driven by varying CO_2 availability relative to biomass, via our different pathways of manipulation, then the most significant factor determining growth rate is likely to be the CO_2 availability (Figure 5a). This linkage is presumably due to the passive diffusion of $[\text{CO}_2]_{\text{aq}}$ into the cell, which determines photosynthesis and therefore growth rate (Bach et al., 2013; Gafar & Schulz, 2018; Monteiro et al., 2016; Sett et al., 2014). It is not surprising that deplete $[\text{CO}_2]$ suppresses *G. huxleyi* growth rates in the CO_2 -limited cultures compared to the CO_2 -replete cultures in our study (Bach, 2011; Riebesell et al., 1993; Sett et al., 2014).

Despite the biggest range in growth rates depending on CO_2 availability in different pathways, isolating the data for a single pathway, yields a significant relationship between $[\text{HCO}_3^-]$ and growth rate in *G. huxleyi* both in CO_2 -limited and CO_2 -replete regimes (Figures 3b–4). One possibility to explain this observation is that *G. huxleyi* made use of HCO_3^- uptake via some Carbon Concentrating Mechanisms (CCMs) in our experiments (Giordano et al., 2005; Kottmeier et al., 2014; Monteiro et al., 2016; Raven et al., 1999) to accumulate CO_2 at the active site of Rubisco and increase rates of carbon fixation (Beardall & Raven, 2013). This may be through the use of HCO_3^- ion exchange transporters, which are solute carrier family 4 (SLC4) proteins (von Dassow et al., 2009; Richier et al., 2011; Taylor et al., 2017) shown to be upregulated under limiting CO_2 . Alternatively, the enzyme carbonic anhydrase (Bach et al., 2015; Richier et al., 2011; Rost et al., 2003; Sikes & Wheeler, 1982), may allow this species to utilize HCO_3^- in CO_2 -limiting conditions to aid growth, or by enhancing calcification through the use of HCO_3^- as substrate to generate H^+ and CO_2 intracellularly or extracellularly (Hoppe et al., 2011). Although not as significant, the same trend of increasing growth rate with HCO_3^- is also apparent in *C. braarudii*, although the increase in growth rate is more significantly correlated with CO_3^{2-} and pH (Figure S4 in Supporting Information S1). To date, it has not been possible to identify an analogous SLC4 transporter supporting HCO_3^- transport in our newly sequenced *C. braarudii* genome (Accession number: PRJNA1321905).

OAE results in a higher pH in seawater. High pH (>8.5) has been shown to depress phytoplankton growth in several studies (Chen & Durbin, 1994; Hansen, 2002; Söderberg & Hansen, 2007; Taraldsvik & Myklesstad, 2000), although evidence suggests that some components of diverse coastal and open ocean phytoplankton communities may be stimulated by pH ~ 9 (Chauhan & Rickaby, 2024; Hinga, 2002; Pedersen & Hansen, 2003), which covers the range of pH values in the CO_2 -limited cultures of this study (Figure S5g in Supporting Information S1). Therefore, species-optima in pH could at least partially be driving the growth rate responses observed in this study, especially in Pathway I. It should be noted that high pH at constant DIC in the modern ocean leads to lower CO_2 availability. Under these conditions, coccolithophores display species specific pH growth optima with the smaller, faster growing species outcompeting the larger slower growing species at higher pH (Chauhan et al., 2024; Chauhan & Rickaby, 2024). But under these conditions of fixed DIC, these optima emerge due to contrasting species thresholds for CO_2 limited growth, such that the larger more carbon demanding species appear more severely limited at higher pH and lower CO_2 availability. In the experiments presented here, where higher TA with higher pH was accompanied by increasing DIC, there appears to be a fertilization of growth in both species, but more significantly in the less carbon demanding *G. huxleyi* (Figure 3b; Figure S4g in Supporting Information S1). This fertilization could be driven by the use of HCO_3^- directly for carbon fixation. Alternatively, since there is no current evidence to support the active uptake of HCO_3^- by *C. braarudii*, then an increased rate of generation of CO_2 in the external media, in proportion to the concentration of ambient HCO_3^- may explain the elevated growth rates. This rate depends on both the concentration of HCO_3^- and H^+ .

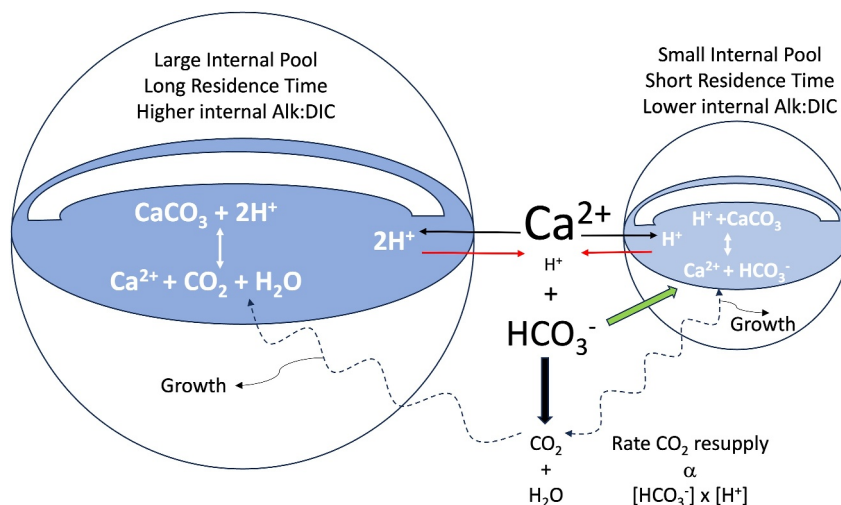


Figure 9. A simplified schematic to demonstrate the hypothetical contrasting use of carbonate chemistry for calcification between the two endmember species in our study as evidenced by the stable isotopic composition of their liths (Branson et al., 2025; Chauhan & Rickaby, 2024). The larger slower-growing and heavily calcified *C. braarudii* has a larger, better buffered internal pool due to the longer residence time of Ca and C inside the cells which relies on a diffusive supply of CO₂ as the carbon source for calcification which re-equilibrates in the internal pool. By contrast, the smaller faster growing and less intensely calcified *G. huxleyi*, although able to use the diffusive supply of CO₂ when sufficiently available, under CO₂-limited growth, has the additional capacity to actively transport HCO₃⁻. Due to the reduced buffering capacity of the smaller internal pool with lower concentrations and shorter residence times of Ca and C, CO₂ can diffuse out of the pool at lower external CO₂ availabilities. The size of the text of the ions is intended to represent the very rough proportional concentrations in the environment. The growth rates of cells are sensitive to the rate of supply of carbon and calcium for photosynthesis and calcification such that ocean alkalinity may inhibit the calcification rate of faster growing cells, when the rate of resupply of carbon for diffusion into the cells is limited by either the external HCO₃⁻ or H⁺ availability.

$$\text{Rate of CO}_2 \text{ production} \sim k [\text{HCO}_3^-] [\text{H}^+]$$

where k is a rate constant. Since *G. huxleyi* has a low PIC/POC (particulate inorganic carbon/particulate organic carbon ratio) any fertilization by OAE acts as positive feedback on carbon draw-down by the short-term carbon cycle due to the fixation rate of carbon outweighing the removal of alkalinity.

4.2. Calcification

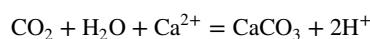
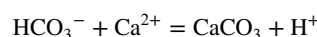
The exact species of the carbonate system which affects calcification in coccolithophores has not been well established. Biochemically, the transporters supplying Ca²⁺ and carbon as the base materials for CaCO₃ production (Bach et al., 2015) are poorly characterized (Tsuji & Yoshida, 2017). When pressure (P), temperature (T) and salinity (S) are constant, there is an inevitable proportionality between CO₃²⁻ and ΩCaCO₃, and HCO₃⁻ and [H⁺] (Bach et al., 2015; Cyronak et al., 2016; Figure 1). ΩCaCO₃ is not a direct physiological driver for calcification, despite correlating well with calcification rates (Waldbusser et al., 2015), but it does control the solubility of CaCO₃ (Zeebe & Wolf-Gladrow, 2001) and therefore could affect how favorable is the environment for calcification.

It has generally been assumed that HCO₃⁻ is the substrate that must be supplied from bulk seawater to the site of calcification. Stable isotopes measured in the liths are suggestive that *G. huxleyi* may use HCO₃⁻ for calcification, but only when external CO₂ supply is limiting. In contrast *C. braarudii* appears to rely on the diffusive supply of CO₂ (Figure 9; Chauhan & Rickaby, 2024). For the *Gephyrocapsids*, increasing ΩCaCO₃ should promote a more favorable environment for calcification and increasing DIC or HCO₃⁻, as the substrate for calcification, should promote more calcification. By contrast, increasing OAE may be more challenging for the Coccolithales since CO₂(aq) is inevitably reduced.

Under CO₂-replete conditions, both *G. huxleyi* and more significantly, *C. braarudii* decreased calcification in response to increasing TA, DIC, and HCO₃⁻ (Figures 3e and 3f, Figure S4 in Supporting Information S1). It is

unlikely that increased concentrations of these carbonate species were inhibiting the calcification rate. The HCO_3^- ion can be ruled out as the only substrate for calcification due to the differing trends of calcification with HCO_3^- availability among our experiments. Calcification rates in *G. huxleyi* increased in proportion to HCO_3^- in CO_2 -depleted experiments (Figure 4e), where these cells may have been upregulating HCO_3^- transport (Mackinder et al., 2011; Trimborn et al., 2014), but calcification decreased in proportion to HCO_3^- in CO_2 replete experiments (Figure 3e). The most likely explanation is that there is an inverse relationship between growth rate and calcification rate in both species under CO_2 replete conditions (Figure 3). The faster the cells fix carbon photosynthetically and divide, the less time each cell has to accumulate carbon into the calcifying vesicle from the external environment. This could result in a rate of carbon demand for calcification that exceeds the rate at which CO_2 can be replenished in the external media, and CO_2 can diffuse into the cells. Given the higher demand for carbon for cellular calcification compared to growth rate in high PIC/POC (particulate inorganic carbon/particulate organic carbon or calcification rate relative to organic carbon fixation rate) species like *C. braarudii* (PIC/POC >1), the decline in calcification rate is more significant than in lower PIC/POC species such as *G. huxleyi*, which also may be supplying HCO_3^- , and have a faster turn-over rate of their internal pool (Chauhan & Rickaby, 2024). In this case, it is the rate at which molecular species diffuse/are transported and are resupplied that is key to keeping pace with calcification rather than their concentration alone. As a result, under high TA conditions, with a higher growth rate, the demand for carbon for calcification became CO_2 limited such that liths were made at a rate faster than their CO_2 supply rate potentially explaining their increasing degree of malformation (Figures 7 and 8). Visual evidence to suggest the role of the diffusive supply of CO_2 for calcification limiting the complete formation of liths under higher pH, low CO_2 can be seen in SEM (Chauhan et al., 2024). Furthermore, an inverse correlation between abundance of *C. pelagicus* and their size-normalized thickness, a proxy for calcification intensity, is evident in high latitude North Atlantic core top sediments, suggestive of a CO_2 limitation of calcification when growing under optimal conditions in the modern environment (González-Lanchas et al., 2025).

$[\text{H}^+]$ is the waste product that must be removed from the site of calcification to bulk seawater during the production of CaCO_3 (Cyronak et al., 2016). It has been proposed that higher external pH should provide an easier environment in which to carry out calcification for either group since high external pH means a low concentration of $[\text{H}^+]$ and thus it should be easier to expel H^+ produced during calcification (Bach et al., 2011, 2013, 2015). Notably, due to the stoichiometry of the reaction, the uptake of HCO_3^- generates only 1 mol of protons per mole of carbon used for calcification, compared to the 2 mol generated by calcification from use of CO_2 :



The expulsion of protons from the cell (in exchange for Ca^{2+}) promotes a high rate of replenishment of CO_2 from HCO_3^- in a microenvironment around the cell (Flynn et al., 2016) for inwards diffusion. It is notable that the doubled expulsion rate associated with the use of CO_2 for calcification, compared to HCO_3^- is insufficient under high alkalinity, low H^+ conditions to supply sufficient CO_2 for growth and calcification demand. Growth appears to be prioritized under these limiting conditions. As a consequence of increased growth but reduced calcification rate/cell, the PIC/POC of both species is likely to decrease with increasing OAE but overall productivity is increased.

Since morphological control is of secondary importance to cellular function (Müller, 2019), under carbonate chemistry conditions where essential functions (i.e., growth, calcification) are perturbed, morphological abnormalities may reflect the turnover of the calcification vesicle occurring at a rate faster than the supply of CO_2 to complete the coccolith and so could be indicative of CO_2 limitation of calcification. Such disruption of coccolith morphology may affect the mechanical resistance of coccolithophores to their predators in the marine environment, making them more vulnerable in the marine ecosystem (Xu et al., 2023).

In CO_2 -deplete conditions, growth rates in *G. huxleyi* were constrained by the instantaneous availability of CO_2 (Figure 5) but it appears that calcification rates, even though significantly depressed relative to their CO_2 -replete experiments, were fertilized at higher TA under these circumstances (Figure 4f). At higher TA, there is a higher availability of HCO_3^- throughout the experiment. This elevated external HCO_3^- , likely fueled calcification, due to upregulation of HCO_3^- transport in these CO_2 limited cells. The carbon supply, from both CO_2 diffusion and

induced HCO_3^- transport can keep pace with the higher growth rates. The lack of change in severe morphological abnormality in these experiments, together with the increase in size of the coccospheres (Figure 6), supports this observation of sufficient carbon for calcification to keep pace with the elevated growth rates with higher TA, in contrast to the CO_2 -replete experiments where carbon demand was much higher.

It is interesting to note the anticorrelation between growth rate and calcification rate in the two species in the CO_2 -replete experiments (Figures 3c and 3f). This suggests that lower calcification rates do not affect or limit growth rates, but that fast growth rates can limit calcification. The two processes do not seem to be mutually beneficial or are independent. Calcification may not act as a CCM, or at least not with a linear relationship which is dependent on the rate of the two processes; it may be an on or off benefit. The lack of impact of morphological disruption on growth rates further suggests that calcification does not feedback on the core cellular process.

4.3. Understanding Coccolithophore Physiology Under OAE

From the data obtained in this study, we have suggested physiological mechanisms to explain the growth and calcification of different species of coccolithophores in response to OAE, and the carbonate system. If both growth rate, and calcification rate are to a first order, dependent on the rate of CO_2 supply to the cells, which is replenished by HCO_3^- and H^+ , at a rate proportional to their concentrations in the external media, and boosted by the rate of H^+ expulsion, then with application of OAE, and assuming equilibration with the air, growth rate of different coccolithophore species will generally be fertilized. Coccolithophores appear to be CO_2 limited under modern ocean conditions (Bolton & Stoll, 2013; Branson et al., 2025; Chauhan & Rickaby, 2024; Chauhan et al., 2024; Rickaby et al., 2010). It is likely that, with air-equilibrated OAE application, smaller species such as *G. huxleyi* and *G. oceanica* with a lower cellular carbon demand, and with the additional ability to utilize HCO_3^- when CO_2 depleted, will experience a greater degree of fertilization, and will outcompete the larger, higher carbon demand species such as *C. braarudii*. Since the Gephyrocapsids have a lower PIC/POC, then their increased rates of carbon fixation and carbon export may have greater positive feedback on CO_2 draw-down, than negative feedback due to alkalinity removal. Similarly, under an OAE induced fertilization, the calcification rate particularly of any high PIC/POC species could be additionally limited by CO_2 supply with morphological abnormalities emerging, leading to their outcompetition by smaller lightly calcified species. This demand for higher alkalinity and HCO_3^- could also explain the more restrictive geographic distribution of *Coccolithus* compared to the *Reticulofenestra* in the modern ocean (Henderiks & Rickaby, 2007; O'Brien et al., 2013). These implications for OAE suggest a latitude dependency to the response. Fertilized growth but with distinct inhibition of calcification may occur at high latitudes where *C. pelagicus* dominate, and reverse the trend toward their increased dominance and calcification in response to anthropogenic CO_2 (Halloran et al., 2008). Further south of 40°N, fertilization of the Gephyrocapsids is more likely.

Overall, it would be expected that the calcification rate of the coccolithophore population will increase due to the fertilized production of cells, which will act to remove some proportion of the added alkalinity from the ocean. This is consistent with periods of the geological past being characterized by high pelagic carbonate production rate when alkalinity input has been high (e.g., Claxton et al., 2022).

The greatest peril for coccolithophores on short timescales, is that the addition of alkalinity has the immediate impact of reducing the $\text{CO}_2(\text{aq})$, and reducing the H^+ s that may be key to the regeneration of CO_2 in the immediate microenvironment around the cells. It is only once the slow process of air-sea exchange has taken place that the CO_2 will be replenished for further use by the biota. For the already CO_2 limited coccolithophores, such a perturbation will reduce their growth and tend to align coccolithophore growth rates with air-sea exchange rates. Unless deployed at levels of alkalinity perturbation below the thresholds shown in this study, it is unlikely that OAE has no impact on calcifying organisms.

4.4. Implications for Ocean Alkalinity Enhancement in the Global Ocean

In this study, the CO_2 -replete culturing experiments with *G. huxleyi* and *C. braarudii* are analogous to an air-equilibrated OAE scenario, and the CO_2 -limited culturing experiments with *G. huxleyi* are analogous to a non-equilibrated OAE scenario. Under CO_2 -replete conditions, *G. huxleyi* slightly decreased its cellular calcification rate in response to raised TA but *C. braarudii* decreased the cellular calcification rate significantly. It is important to bear in mind that the levels of TA in this study are raised to levels far above what is likely for early field trials and commercial deployments. However, even if *G. huxleyi* calcification per cell does not change by a

large amount, the growth rate of *G. huxleyi* significantly increases with the supply of HCO_3^- in our study, even in our lowest alkalinity treatments at TA $\sim 3,000 \mu\text{mol kg}^{-1}$ ($\sim 500 \mu\text{mol kg}^{-1}$ above control conditions). A larger population size of *G. huxleyi* would result from this, and so by virtue of there being a higher number of cells calcifying, the overall amount of calcification from the *G. huxleyi* population might be significantly increased, depending on the balance between increase of population size versus any change in calcification rate. This situation could be analogous to the high alkalinity Black Sea ($\sim 3,300 \mu\text{mol kg}^{-1}$) where blooms of *G. huxleyi* are ubiquitous (Kopelevich et al., 2014, 2020) and population levels of calcification are extremely high, as evidenced by the thick layers of calcareous ooze overlying bottom sediments (Hay, 1988). Further, there were increases in coccolithophore calcification during the higher alkalinity ocean of the last glacial maximum (Beaufort et al., 2011) and the increased weathering input of the Eocene climatic optimum (Claxton et al., 2022). A similar value for an upper threshold for alkalinity addition (of $< 1,000 \mu\text{mol/kg}$ additional alkalinity) has been proposed to avoid inorganic calcium carbonate precipitation (Hartmann et al., 2023; Suitner et al., 2023). This suggests that a convergence on operating boundaries is beginning to emerge from both an inorganic and biotic perspective.

G. huxleyi cellular calcification rates and quota may however increase in non-equilibrated OAE scenarios, resulting in CO_2 re-release after drawdown into the surface ocean from alkalinity addition. However, probably, non-equilibrated OAE scenarios will only occur on initial point-source additions of alkalinity, so any possible re-release of CO_2 would be short-lived, and it is likely that once the surface ocean and atmosphere have equilibrated that coccolithophore calcification would then decrease or remain the same relative to control conditions. Additionally, our laboratory experiments were conducted under nutrient-replete conditions, but calcification response to OAE may be limited by lack of available nutrients in natural environments (Müller et al., 2017; Zhang & Gao, 2021).

In the global ocean, it is not just the process of calcification that induces changes in the carbon cycle. Although PIC:POC was not determined in our study, we must note that a change of PIC:POC values of coccolithophores would also affect the overall carbon fixation. It was predicted that if PIC:POC < 1 , organic carbon export would offset the CO_2 emission from the counter carbonate pump (Renforth & Henderson, 2017). This would need to be further studied to answer the question of to what extent the interaction between PIC and POC formation will impact overall carbon drawdown during OAE. Calcium carbonate formation by biota contributes to the ballasting of organic carbon particulate matter to the deep ocean (Honjo et al., 2008; Rost & Riebesell, 2004; Ziveri et al., 2007). Therefore, it follows that more calcite formation could lead to more ballasting and more organic carbon export to the deep ocean. This could have wide-ranging impacts on global carbon cycling. Again, while showing evidence for calcification responses in coccolithophores, we reiterate that our study still leaves unanswered questions concerning the interaction between biotic organic and inorganic carbon formation during OAE. This is particularly relevant given that our data were obtained from batch cultures experiments, which may not fully capture natural bloom dynamics, such as the impacts from nutrient competition and grazing pressure. Further research is necessary to validate our experimental findings via chemostat experiments, and mesocosms as well as interrogation of field analysis and the geological record at times in the geological past when ocean alkalinity was elevated (Subhas et al., 2023).

5. Conclusions

Increased ocean alkalinity has a greater impact on *G. huxleyi* growth and *C. braarudii* calcification processes. The growth and calcification responses of the two species to the carbonate chemistries resulting from OAE suggest that each species is CO_2 -limited under modern conditions and growth is fertilized by additional alkalinity and DIC. The fertilization arises from an increase in the HCO_3^- ion under higher alkalinity leading to either greater availability of the substrate or a higher rate of CO_2 resupply as the coccolithophores utilize CO_2 during photosynthesis and maintain high growth rates. The difference in their calcification response relates to the much greater carbon demand of the larger *C. braarudii* cells, and their reliance on CO_2 for calcification which leads to significantly decreased calcification in this species under OAE compared to *G. huxleyi* which has the ability to utilize HCO_3^- at low CO_2 . Our results indicate that there is a possibility of re-release of CO_2 during OAE due to enhanced growth of calcifying coccolithophores, in response to greater carbon supply rate, leading to increased calcification rates and removal of the alkalinity. High levels of alkalinity enhancement may induce severe coccolith malformation due to the fertilized growth rate of the cells, requiring a greater supply rate of CO_2 for the associated enhanced rates of calcification resulting in CO_2 limitation of calcification. This study examines alkalinity enhancement scenarios at much more extreme perturbations than are likely during early field trials and

commercial deployments of OAE, and so we advocate based on our results for careful strategic planning during implementation of OAE, to ensure any carbonate chemistry perturbations are kept within the levels at which we observed significant growth responses in our study (responses observed at $\sim 3,000 \mu\text{mol kg}^{-1}$), both to ensure safe ecosystem boundaries are maintained, and any reduction in the efficacy of OAE is avoided.

Conflict of Interest

The authors declare no conflicts of interest relevant to this study.

Data Availability Statement

All experimental data supporting the findings of this study are available within the paper and its Supporting Information S1.

The datasets are deposited in the Zenodo at DOI: <https://doi.org/10.5281/zenodo.17479763>.

Data analysis and figures were generated using R (Version 4.2.2), available at <https://www.r-project.org/>, and GraphPad Prism 9.4, accessible at <https://www.graphpad.com/>.

Acknowledgments

S.G acknowledges financial support from the Natural Environment Research Council (NERC) project NE/P019536/1. Q.Z. acknowledges funding support from Southern Marine Science and Engineering Guangdong Laboratory Independent Research grant SML2021SP204, Research Grants Council of the Hong Kong Special Administrative Region, China (26304723 and C6006-22E), and CORE. CORE is a joint research centre for ocean research between Laoshan Laboratory and HKUST. R.E.M.R acknowledges funding support from the European Research Council (ERC) under the European Union's Horizon 2020 research and innovation program (SCOOBI project, grant agreement no. 101019146; RER) and from the Natural Environment Research Council (NERC; PUGCA project, award NE/V011049/1; RER). Electron microscopy was performed in the Sir William Dunn School EM facility at the University of Oxford, and we are grateful to Dr Errin Johnson for sample preparation and advice. We thank Joseph Snow and Jonathan Erez for their generous help and invaluable discussion, and the anonymous reviewers for their help in improving the quality of our manuscript.

References

- Albright, R., Caldeira, L., Hosfelt, J., Kwiatkowski, L., Maclaren, J. K., Mason, B. M., et al. (2016). Reversal of ocean acidification enhances net coral reef calcification. *Nature*, *531*(7594), 362–365. <https://doi.org/10.1038/nature17155>
- Bach, L. T. (2024). The additionality problem of ocean alkalinity enhancement. *Biogeosciences*, *21*(1), 261–277. <https://doi.org/10.5194/bg-21-261-2024>
- Bach, L. T., Gill, S. J., Rickaby, R. E. M., Gore, S., & Renforth, P. (2019). CO₂ removal with enhanced weathering and ocean alkalinity enhancement: Potential risks and co-benefits for marine pelagic ecosystems. *Frontiers in Climate*, *1*(October), 7. <https://doi.org/10.3389/fclim.2019.00007>
- Bach, L. T., Ho, D. T., Boyd, P. W., & Tyka, M. D. (2023). Toward a consensus framework to evaluate air–sea CO₂ equilibration for marine CO₂ removal. *Limnology and Oceanography Letters*, *8*(5), 685–691. <https://doi.org/10.1002/lol2.10330>
- Bach, L. T., Mackinder, L. C. M., Schulz, K. G., Wheeler, G., Schroeder, D. C., Brownlee, C., & Riebesell, U. (2013). Dissecting the impact of CO₂ and pH on the mechanisms of photosynthesis and calcification in the coccolithophore *Emiliania huxleyi*. *New Phytologist*, *199*(1), 121–134. <https://doi.org/10.1111/nph.12225>
- Bach, L. T., Riebesell, U., Gutowska, M. A., Federwisch, L., & Schulz, K. G. (2015). A unifying concept of coccolithophore sensitivity to changing carbonate chemistry embedded in an ecological framework. *Progress in Oceanography*, *135*, 125–138. <https://doi.org/10.1016/j.pocean.2015.04.012>
- Bach, L. T., Riebesell, U., & Schulz, K. G. (2011). Distinguishing between the effects of ocean acidification and ocean carbonation in the coccolithophore *Emiliania huxleyi*. *Limnology & Oceanography*, *56*(6), 2040–2050. <https://doi.org/10.4319/lo.2011.56.6.2040>
- Beardall, J., & Raven, J. A. (2013). Calcification and ocean acidification: New insights from the coccolithophore *Emiliania huxleyi*. *New Phytologist*, *199*(1), 1–3. <https://doi.org/10.1111/nph.12297>
- Beaufort, L., Probert, I., de Garidel-Thoron, T., Bendif, E. M., Ruiz-Pino, D., Metzl, N., et al. (2011). Sensitivity of coccolithophores to carbonate chemistry and ocean acidification. *Nature*, *476*(7358), 80–83. <https://doi.org/10.1038/nature10295>
- Bednaršek, N., Pelletier, G., van de Mortel, H., García-Reyes, M., Feely, R., & Dickson, A. (2024). Unifying framework for assessing sensitivity for marine calcifiers to ocean alkalinity enhancement identifies winners, losers and biological thresholds—Importance of caution with precautionary principle. <https://doi.org/10.5194/egusphere-2024-947>
- Bendif, E. M., Nevado, B., Wong, E. L. Y., Hagino, K., Probert, I., Young, J. R., et al. (2019). Repeated species radiations in the recent evolution of the key marine phytoplankton lineage Gephyrocapsa. *Nature Communications*, *10*(1), 1–9. <https://doi.org/10.1038/s41467-019-12169-7>
- Bendif, E. M., Probert, I., Archontikis, O. A., Young, J. R., Beaufort, L., Rickaby, R. E., & Filatov, D. (2023). Rapid diversification underlying the global dominance of a cosmopolitan phytoplankton. *The ISME Journal*, *17*(4), 630–640. <https://doi.org/10.1038/s41396-023-01365-5>
- Blanco-Ameijeiras, S., Lebrato, M., Stoll, H. M., Iglesias-Rodriguez, D., Müller, M. N., Méndez-Vicente, A., & Oschlies, A. (2016). Phenotypic variability in the coccolithophore *Emiliania huxleyi*. *PLoS One*, *11*(6), e0157697. <https://doi.org/10.1371/journal.pone.0157697>
- Bolton, C. T., & Stoll, H. M. (2013). Late Miocene threshold response of marine algae to carbon dioxide limitation. *Nature*, *500*(7464), 558–562. <https://doi.org/10.1038/nature12448>
- Branson, O., Chauhan, N., Evans, D., Foster, G. L., & Rickaby, R. E. M. (2025). Geochemical tracers of biomineralization processes. In *Treatise on geochemistry* (pp. 177–235). Elsevier. <https://doi.org/10.1016/B978-0-323-99762-1.00128-5>
- Buitenhuis, E. T., De Baar, H. J. W., & Veldhuis, M. J. W. (1999). Photosynthesis and calcification by *Emiliania huxleyi* (Prymnesiophyceae) as a function of inorganic carbon species. *Journal of Phycology*, *35*(5), 949–959. <https://doi.org/10.1046/j.1529-8817.1999.3550949.x>
- Chauhan, N., Dedman, C. J., Baldreki, C., Dowle, A. A., Larson, T. R., & Rickaby, R. E. M. (2024). Contrasting species-specific stress response to environmental pH determines the fate of coccolithophores in future oceans. *Marine Pollution Bulletin*, *209*, 117136. <https://doi.org/10.1016/j.marpolbul.2024.117136>
- Chauhan, N., & Rickaby, R. E. M. (2024). Size-dependent dynamics of the internal carbon pool drive isotopic vital effects in calcifying phytoplankton. *Geochimica et Cosmochimica Acta*, *373*, 35–51. <https://doi.org/10.1016/j.gca.2024.03.033>
- Chen, C., & Durbin, E. (1994). Effects of pH on the growth and carbon uptake of marine phytoplankton. *Marine Ecology Progress Series*, *109*(1), 83–94. <https://doi.org/10.3354/meps109083>
- Chisholm, J. R. M., & Gattuso, J.-P. (1991). Validation of the alkalinity anomaly technique for investigating calcification of photosynthesis in coral reef communities. *Limnology & Oceanography*, *36*(6), 1232–1239. <https://doi.org/10.4319/lo.1991.36.6.1232>
- Claxton, L. M., McClelland, H. L. O., Hermoso, M., & Rickaby, R. E. M. (2022). Eocene emergence of highly calcifying coccolithophores despite declining atmospheric CO₂. *Nature Geoscience*, *15*(10), 826–831. <https://doi.org/10.1038/s41561-022-01006-0>

- Cohen, S., Krueger, T., & Fine, M. (2017). Measuring coral calcification under ocean acidification: Methodological considerations for the ^{45}C -uptake and total alkalinity anomaly technique. *PeerJ*, 5(9), e3749. <https://doi.org/10.7717/peerj.3749>
- Cook, S. S., Whittock, L., Wright, S. W., & Hallegraeff, G. M. (2011). Photosynthetic pigment and genetic differences between two Southern Ocean morphotypes of *Emiliania huxleyi* (Haptophyta). *Journal of Phycology*, 47(3), 615–626. <https://doi.org/10.1111/j.1529-8817.2011.00992.x>
- Cyronak, T., Schulz, K. G., & Jokić, P. L. (2016). The Omega myth: What really drives lower calcification rates in an acidifying ocean. *ICES Journal of Marine Science*, 73(3), 558–562. <https://doi.org/10.1093/icesjms/fsv075>
- Daniels, C. J., Sheward, R. M., & Poulton, A. J. (2014). Biogeochemical implications of comparative growth rates of *Emiliania huxleyi* and *Coccolithus* species. *Biogeosciences*, 11(23), 6915–6925. <https://doi.org/10.5194/bg-11-6915-2014>
- de Vries, J., Monteiro, F., Wheeler, G., Poulton, A., Godrić, J., Cerino, F., et al. (2021). Haplo-diplontic life cycle expands coccolithophore niche. *Biogeosciences*, 18(3), 1161–1184. <https://doi.org/10.5194/bg-18-1161-2021>
- Doney, S. C., Fabry, V. J., Feely, R. A., & Kleypas, J. A. (2009). Ocean acidification: The other CO_2 problem. *Annual Review of Marine Science*, 1(1), 169–192. <https://doi.org/10.1146/annurev.marine.010908.163834>
- Dupont, S., & Metian, M. (2023). General considerations for experimental research on ocean alkalinity enhancement. *State of the Planet, 2-oae2023*, 1–11. <https://doi.org/10.5194/sp-2-oae2023-4-2023>
- Faucher, G., Haunost, M., Paul, A. J., Tietz, A. U. C., & Riebesell, U. (2025). Growth response of *Emiliania huxleyi* to ocean alkalinity enhancement. *Biogeosciences*, 22(2), 405–415. <https://doi.org/10.5194/bg-22-405-2025>
- Feng, E. Y., Koeve, W., Keller, D. P., & Oschlies, A. (2017). Model-Based assessment of the CO_2 sequestration potential of coastal Ocean alkalization. *Earth's Future*, 5(12), 1252–1266. <https://doi.org/10.1002/2017EF000659>
- Flynn, K. J., Clark, D. R., & Wheeler, G. (2016). The role of coccolithophore calcification in bioengineering their environment. *Proceedings of the Royal Society B: Biological Sciences*, 283(1833), 20161099. <https://doi.org/10.1098/rspb.2016.1099>
- Fuss, S., Canadell, J. G., Peters, G. P., Tavoni, M., Andrew, R. M., Ciais, P., et al. (2014). Betting on negative emissions. *Nature Climate Change*, 4(10), 850–853. <https://doi.org/10.1038/nclimate2392>
- Gafar, N. A., & Schulz, K. G. (2018). A three-dimensional niche comparison of *Emiliania huxleyi* and *Gephyrocapsa oceanica*: Reconciling observations with projections. *Biogeosciences*, 15(11), 3541–3560. <https://doi.org/10.5194/bg-15-3541-2018>
- Gagem, A., Manley, J., & Kapsenberg, L. (2022). Ocean-based carbon dioxide removal: A new frontier in the blue economy. *Marine Technology Society Journal*, 56(1), 40–48. <https://doi.org/10.4031/MTSJ.56.1.15>
- Gately, J. A., Kim, S. M., Jin, B., Brzezinski, M. A., & Iglesias-Rodriguez, M. D. (2023). Coccolithophores and diatoms resilient to ocean alkalinity enhancement: A glimpse of hope? *Science Advances*, 9(24), eadg6066. <https://doi.org/10.1126/sciadv.adg6066>
- Gattuso, J.-P., Magnan, A. K., Bopp, L., Cheung, W. W. L., Duarte, C. M., Hinkel, J., et al. (2018). Ocean solutions to address climate change and its effects on marine ecosystems. *Frontiers in Marine Science*, 5(OCT), 337. <https://doi.org/10.3389/fmars.2018.00337>
- GESAMP. (2019). High level review of a wide range of proposed marine geoengineering techniques. In *GESAMP reports and studies* (Vol. 98).
- Giordano, M., Beardall, J., & Raven, J. A. (2005). CO_2 concentrating mechanisms in ALGAE: Mechanisms, Environmental Modulation, and Evolution. *Annual Review of Plant Biology*, 56(1), 99–131. <https://doi.org/10.1146/annurev.arplant.56.032604.144052>
- González-Lanchas, A., Karl-Heinz, B., Heather, M. S., José-Abel, F., Miguel Angel, F., & Rosalind, E. M. R. (2025). Coccolithophore calcite production from nanofossil records. <https://doi.org/10.5194/egusphere-egu25-10717>
- Gore, S., Renforth, P., & Perkins, R. (2019). The potential environmental response to increasing ocean alkalinity for negative emissions. *Mitigation and Adaptation Strategies for Global Change*, 24(7), 1191–1211. <https://doi.org/10.1007/s11027-018-9830-z>
- Guillard, R. R. L., & Hargraves, P. E. (1993). *Süchochrysis immobilis* is a diatom, not a chrysochyte. *Phycologia*, 32(3), 234–236. <https://doi.org/10.2216/i0031-8884-32-3-234.1>
- Halloran, P. R., Hall, I. R., Colmenero-Hidalgo, E., & Rickaby, R. E. M. (2008). Evidence for a multi-species coccolith volume change over the past two centuries: Understanding a potential ocean acidification response. *Biogeosciences*, 5(6), 1651–1655. <https://doi.org/10.5194/bg-5-1651-2008>
- Hansen, P. (2002). Effect of high pH on the growth and survival of marine phytoplankton: Implications for species succession. *Aquatic Microbial Ecology*, 28(3), 279–288. <https://doi.org/10.3354/ame028279>
- Harlay, J., Borges, A. V., Van Der Zee, C., Delille, B., Godoi, R. H. M., Schiettecatte, L.-S., et al. (2010). Biogeochemical study of a coccolithophore bloom in the northern Bay of Biscay (NE Atlantic Ocean) in June 2004. *Progress in Oceanography*, 86(3–4), 317–336. <https://doi.org/10.1016/j.pocean.2010.04.029>
- Hartmann, J., Suitner, N., Lim, C., Schneider, J., Marín-Samper, L., Aristegui, J., et al. (2023). Stability of alkalinity in ocean alkalinity enhancement (OAE) approaches—Consequences for durability of CO_2 storage. *Biogeosciences*, 20(4), 781–802. <https://doi.org/10.5194/bg-20-781-2023>
- Hartmann, J., West, A. J., Renforth, P., Köhler, P., De La Rocha, C. L., Wolf-Gladrow, D. A., et al. (2013). Enhanced chemical weathering as a geoengineering strategy to reduce atmospheric carbon dioxide, supply nutrients, and mitigate ocean acidification. *Reviews of Geophysics*, 51(2), 113–149. <https://doi.org/10.1002/rog.20004>
- Hay, B. J. (1988). Sediment accumulation in the central western Black Sea over the past 5100 years. *Paleoceanography*, 3(4), 491–508. <https://doi.org/10.1029/PA003i004p00491>
- Henderiks, J., & Rickaby, R. E. M. (2007). A coccolithophore concept for constraining the Cenozoic carbon cycle. *Biogeosciences*, 4(3), 323–329. <https://doi.org/10.5194/bg-4-323-2007>
- Hermoso, M. (2015). Control of ambient pH on growth and stable isotopes in phytoplanktonic calcifying algae. *Paleoceanography*, 30(8), 1100–1112. <https://doi.org/10.1002/2015PA002844>
- Hermoso, M., Horner, T. J., Minoletti, F., & Rickaby, R. E. M. (2014). Constraints on the vital effect in coccolithophore and dinoflagellate calcite by oxygen isotopic modification of seawater. *Geochimica et Cosmochimica Acta*, 141, 612–627. <https://doi.org/10.1016/j.gca.2014.05.002>
- Hinga, K. (2002). Effects of pH on coastal marine phytoplankton. *Marine Ecology Progress Series*, 238, 281–300. <https://doi.org/10.3354/meps238281>
- Honjo, S., Manganini, S. J., Krishfield, R. A., & Francois, R. (2008). Particulate organic carbon fluxes to the ocean interior and factors controlling the biological pump: A synthesis of global sediment trap programs since 1983. *Progress in Oceanography*, 76(3), 217–285. <https://doi.org/10.1016/j.pocean.2007.11.003>
- Hoppe, C. J. M., Langer, G., & Rost, B. (2011). *Emiliania huxleyi* shows identical responses to elevated $p\text{CO}_2$ in TA and DIC manipulations. *Journal of Experimental Marine Biology and Ecology*, 406(1–2), 54–62. <https://doi.org/10.1016/j.jembe.2011.06.008>
- Iglesias-Rodriguez, M. D., Halloran, P. R., Rickaby, R. E. M., Hall, I. R., Colmenero-Hidalgo, E., Gittins, J. R., et al. (2008). Phytoplankton calcification in a High- CO_2 world. *Science*, 320(5874), 336–340. <https://doi.org/10.1126/science.1154122>

- Iglesias-Rodríguez, M. D., Rickaby, R. E. M., Singh, A., & Gately, J. A. (2023). Laboratory experiments in ocean alkalinity enhancement research. *State of the Planet, 2-oae2023*(July), 1–18. <https://doi.org/10.5194/sp-2-oae2023-5-2023>
- Ilyina, T., Wolf-Gladrow, D., Munhoven, G., & Heinze, C. (2013). Assessing the potential of calcium-based artificial ocean alkalization to mitigate rising atmospheric CO₂ and ocean acidification. *Geophysical Research Letters*, *40*(22), 5909–5914. <https://doi.org/10.1002/2013GL057981>
- IPCC. (2001). The carbon cycle and atmospheric carbon dioxide. In *Climate Change 2001: The Scientific Basis* (pp. 183–237). <https://doi.org/10.1256/004316502320517344>
- Isometric. (2024). Ocean alkalinity enhancement from coastal outfalls.
- Kheshgi, H. S. (1995). Sequestering atmospheric carbon dioxide by increasing ocean alkalinity. *Energy*, *20*(9), 915–922. [https://doi.org/10.1016/0360-5442\(95\)00035-F](https://doi.org/10.1016/0360-5442(95)00035-F)
- Köhler, P., Abrams, J. F., Völker, C., Hauck, J., & Wolf-Gladrow, D. A. (2013). Geoengineering impact of open ocean dissolution of olivine on atmospheric CO₂, surface ocean pH and marine biology. *Environmental Research Letters*, *8*(1), 014009. <https://doi.org/10.1088/1748-9326/8/1/014009>
- Köhler, P., Hartmann, J., & Wolf-Gladrow, D. A. (2010). Geoengineering potential of artificially enhanced silicate weathering of olivine. *Proceedings of the National Academy of Sciences*, *107*(47), 20228–20233. <https://doi.org/10.1073/pnas.1000545107>
- Kopelevich, O., Burenkov, V., Sheberstov, S., Vazyulya, S., Kravchishina, M., Pautova, L., et al. (2014). Satellite monitoring of coccolithophore blooms in the Black Sea from ocean color data. *Remote Sensing of Environment*, *146*, 113–123. <https://doi.org/10.1016/j.rse.2013.09.009>
- Kopelevich, O., Sheberstov, S., & Vazyulya, S. (2020). Effect of a coccolithophore bloom on the underwater light field and the Albedo of the water column. *Journal of Marine Science and Engineering*, *8*(6), 456. <https://doi.org/10.3390/jmse8060456>
- Kottmeier, D. M., Rokitta, S. D., & Rost, B. (2016). Acidification, not carbonation, is the major regulator of carbon fluxes in the coccolithophore *Emiliana huxleyi*. *New Phytologist*, *211*(1), 126–137. <https://doi.org/10.1111/nph.13885>
- Kottmeier, D. M., Rokitta, S. D., Tortell, P. D., & Rost, B. (2014). Strong shift from HCO₃[−] to CO₂ uptake in *Emiliana huxleyi* with acidification: New approach unravels acclimation versus short-term pH effects. *Photosynthesis Research*, *121*(2–3), 265–275. <https://doi.org/10.1007/s1120-014-9984-9>
- Kubryakov, A. A., Mikaelyan, A. S., & Stanichny, S. V. (2019). Summer and winter coccolithophore blooms in the Black Sea and their impact on production of dissolved organic matter from Bio-Argo data. *Journal of Marine Systems*, *199*, 103220. <https://doi.org/10.1016/j.jmarsys.2019.103220>
- Lee, J., & Morse, J. W. (2010). Influences of alkalinity and pCO₂ on CaCO₃ nucleation from estimated Cretaceous composition seawater representative of “calcite seas”. *Geology*, *38*(2), 115–118. <https://doi.org/10.1130/G30537.1>
- Mackinder, L., Wheeler, G., Schroeder, D., von Dassow, P., Riebesell, U., & Brownlee, C. (2011). Expression of biomineralization-related ion transport genes in *Emiliana huxleyi*. *Environmental Microbiology*, *13*(12), 3250–3265. <https://doi.org/10.1111/j.1462-2920.2011.02561.x>
- Mayers, T. J., Bramucci, A. R., Yakimovich, K. M., & Case, R. J. (2016). A bacterial pathogen displaying temperature-enhanced virulence of the microalga *Emiliana huxleyi*. *Frontiers in Microbiology*, *7*(JUN), 892. <https://doi.org/10.3389/fmicb.2016.00892>
- Meyer, J., & Riebesell, U. (2015). Reviews and Syntheses: Responses of coccolithophores to ocean acidification: A meta-analysis. *Biogeosciences*, *12*(6), 1671–1682. <https://doi.org/10.5194/bg-12-1671-2015>
- Monteiro, F. M., Bach, L. T., Brownlee, C., Bown, P., Rickaby, R. E. M., Poulton, A. J., et al. (2016). Why marine phytoplankton calcify. *Science Advances*, *2*(7), e1501822. <https://doi.org/10.1126/sciadv.1501822>
- Müller, M. N. (2019). On the genesis and function of coccolithophore calcification. *Frontiers in Marine Science*, *6*(FEB), 49. <https://doi.org/10.3389/fmars.2019.00049>
- Müller, M. N., Trull, T. W., & Hallegraeff, G. M. (2017). Independence of nutrient limitation and carbon dioxide impacts on the Southern Ocean coccolithophore *Emiliana huxleyi*. *The ISME Journal*, *11*(8), 1777–1787. <https://doi.org/10.1038/ismej.2017.53>
- O’Brien, C. J., Peloquin, J. A., Vogt, M., Heinle, M., Gruber, N., Ajani, P., et al. (2013). Global marine plankton functional type biomass distributions: Coccolithophores. *Earth System Science Data*, *5*(2), 259–276. <https://doi.org/10.5194/essd-5-259-2013>
- O’Brien, C. J., Vogt, M., & Gruber, N. (2016). Global coccolithophore diversity: Drivers and future change. *Progress in Oceanography*, *140*, 27–42. <https://doi.org/10.1016/j.pocean.2015.10.003>
- Oschlies, A., Bach, L. T., Rickaby, R. E. M., Satterfield, T., Webb, R., & Gattuso, J.-P. (2023). Climate targets, carbon dioxide removal, and the potential role of ocean alkalinity enhancement. *State of the Planet, 2-oae2023*, 1–9. <https://doi.org/10.5194/sp-2-oae2023-1-2023>
- Pedersen, F., & Hansen, P. (2003). Effects of high pH on a natural marine planktonic community. *Marine Ecology Progress Series*, *260*, 19–31. <https://doi.org/10.3354/meps260019>
- Perrin, L., Probert, I., Langer, G., & Aloisi, G. (2016). Growth of the coccolithophore *Emiliana huxleyi* in light- and nutrient-limited batch reactors: Relevance for the BIOSOPE deep ecological niche of coccolithophores. *Biogeosciences*, *13*(21), 5983–6001. <https://doi.org/10.5194/bg-13-5983-2016>
- Pierrot, D. E., Wallace, D. W. R., & Lewis, E. (2011). *MS Excel Program developed for CO₂ system calculations*. Carbon Dioxide Information Analysis Center. https://doi.org/10.3334/CDIAC/otg.CO2SYS_XLS.CDIAC105a
- Poulton, A. J., Adey, T. R., Balch, W. M., & Holligan, P. M. (2007). Relating coccolithophore calcification rates to phytoplankton community dynamics: Regional differences and implications for carbon export. *Deep Sea Research Part II: Topical Studies in Oceanography*, *54*(5–7), 538–557. <https://doi.org/10.1016/j.dsr2.2006.12.003>
- Raven, J. A., Evans, M. C. W., & Korb, R. E. (1999). The role of trace metals in photosynthetic electron transport in O₂-evolving organisms. *Photosynthesis Research*, *60*(2–3), 111–150. <https://doi.org/10.1023/A:1006282714942>
- Renforth, P., & Henderson, G. (2017). Assessing ocean alkalinity for carbon sequestration. *Reviews of Geophysics*, *55*(3), 636–674. <https://doi.org/10.1002/2016RG000533>
- Richier, S., Fiorini, S., Kerros, M.-E., von Dassow, P., & Gattuso, J.-P. (2011). Response of the calcifying coccolithophore *Emiliana huxleyi* to low pH/high pCO₂: From physiology to molecular level. *Marine Biology*, *158*(3), 551–560. <https://doi.org/10.1007/s00227-010-1580-8>
- Rickaby, R. E. M., Henderiks, J., & Young, J. N. (2010). Perturbing phytoplankton: Response and isotopic fractionation with changing carbonate chemistry in two coccolithophore species. *Climate of the Past*, *6*(6), 771–785. <https://doi.org/10.5194/cp-6-771-2010>
- Rickaby, R. E. M., Schrag, D. P., Zondervan, I., & Riebesell, U. (2002). Growth rate dependence of Sr incorporation during calcification of *Emiliana huxleyi*. *Global Biogeochemical Cycles*, *16*(1), 6–1. <https://doi.org/10.1029/2001GB001408>
- Riebesell, U., Fabry, V. J., & Hansson, L. (2010). *Guide to best practices for ocean acidification research and data reporting*. European Commission. <https://doi.org/10.2777/58454>
- Riebesell, U., Wolf-Gladrow, D. A., & Smetacek, V. (1993). Carbon dioxide limitation of marine phytoplankton growth rates. *Nature*, *361*(6409), 249–251. <https://doi.org/10.1038/361249a0>

- Rigual-Hernández, A. S., Trull, T. W., Flores, J. A., Nodder, S. D., Eriksen, R., Davies, D. M., et al. (2020). Full annual monitoring of Subantarctic *Emiliana huxleyi* populations reveals highly calcified morphotypes in high-CO₂ winter conditions. *Scientific Reports*, *10*(1), 2594. <https://doi.org/10.1038/s41598-020-59375-8>
- Rost, B., & Riebesell, U. (2004). Coccolithophores and the biological pump: Responses to environmental changes. In *Coccolithophores* (pp. 99–125). Springer. https://doi.org/10.1007/978-3-662-06278-4_5
- Rost, B., Riebesell, U., Burkhardt, S., & Sültemeyer, D. (2003). Carbon acquisition of bloom-forming marine phytoplankton. *Limnology & Oceanography*, *48*(1), 55–67. <https://doi.org/10.4319/lo.2003.48.1.0055>
- Roy, R. N., Roy, L. N., Lawson, M., Vogel, K. M., Porter Moore, C., Davis, W., & Millero, F. J. (1993). Thermodynamics of the dissociation of boric acid in seawater at S = 35 from 0 to 55°C. *Marine Chemistry*, *44*(2–4), 243–248. [https://doi.org/10.1016/0304-4203\(93\)90206-4](https://doi.org/10.1016/0304-4203(93)90206-4)
- Sarmiento, J. L., & Gruber, N. (2013). *Ocean biogeochemical dynamics*. Ocean biogeochemical dynamics. Princeton University Press. <https://doi.org/10.2307/j.ct3f9xqx>
- Sett, S., Bach, L. T., Schulz, K. G., Koch-Klavnsen, S., Lebrato, M., & Riebesell, U. (2014). Temperature modulates coccolithophorid sensitivity of growth, photosynthesis and calcification to increasing seawater pCO₂. *PLoS One*, *9*(2), e88308. <https://doi.org/10.1371/journal.pone.0088308>
- Shafiee, R. T., Diver, P. J., Snow, J. T., Zhang, Q., & Rickaby, R. E. M. (2021). Marine ammonia-oxidising archaea and bacteria occupy distinct iron and copper niches. *ISME Communications*, *1*(1), 1. <https://doi.org/10.1038/s43705-021-00001-7>
- Sikes, C. S., Roer, R. D., & Wilbur, K. M. (1980). Photosynthesis and coccolith formation: Inorganic carbon sources and net inorganic reaction of deposition. *Limnology & Oceanography*, *25*(2), 248–261. <https://doi.org/10.4319/lo.1980.25.2.0248>
- Sikes, C. S., & Wheeler, A. P. (1982). Carbonic anhydrase and carbon fixation in coccolithophores. *Journal of Phycology*, *18*(3), 423–426. <https://doi.org/10.1111/j.1529-8817.1982.tb03205.x>
- Silverman, J., Lazar, B., & Erez, J. (2007). Effect of aragonite saturation, temperature, and nutrients on the community calcification rate of a coral reef. *Journal of Geophysical Research*, *112*(C5), C05004. <https://doi.org/10.1029/2006JC003770>
- Sønderberg, L., & Hansen, P. (2007). Growth limitation due to high pH and low inorganic carbon concentrations in temperate species of the dinoflagellate genus *Ceratium*. *Marine Ecology Progress Series*, *351*, 103–112. <https://doi.org/10.3354/meps07146>
- Stevenson, E. I., Hermoso, M., Rickaby, R. E. M., Tyler, J. J., Minoletti, F., Parkinson, I. J., et al. (2014). Controls on stable strontium isotope fractionation in coccolithophores with implications for the marine Sr cycle. *Geochimica et Cosmochimica Acta*, *128*, 225–235. <https://doi.org/10.1016/j.gca.2013.11.043>
- Subhas, A. V., Lehmann, N., & Rickaby, R. E. M. (2023). Natural analogs to ocean alkalinity enhancement. *State of the Planet, 2-oae2023*, 1–17. <https://doi.org/10.5194/sp-2-oae2023-8-2023>
- Subhas, A. V., Marx, L., Reynolds, S., Flohr, A., Mawji, E. W., Brown, P. J., & Cael, B. B. (2022). Microbial ecosystem responses to alkalinity enhancement in the North Atlantic Subtropical Gyre. *Frontiers in Climate*, *4*, 784997. <https://doi.org/10.3389/fclim.2022.784997>
- Suitner, N., Faucher, G., Lim, C., Schneider, J., Moras, C. A., Riebesell, U., & Hartmann, J. (2023). Ocean alkalinity enhancement approaches and the predictability of runaway precipitation processes—Results of an experimental study to determine critical alkalinity ranges for safe and sustainable application scenarios. <https://doi.org/10.5194/egusphere-2023-2611>
- Taraldsvik, M., & Mykkestad, S. (2000). The effect of pH on growth rate, biochemical composition and extracellular carbohydrate production of the marine diatom *Skeletonema costatum*. *European Journal of Phycology*, *35*(2), 189–194. <https://doi.org/10.1080/09670260010001735781>
- Taylor, A. R., Brownlee, C., & Wheeler, G. (2017). Coccolithophore cell biology: Chalking up progress. *Annual Review of Marine Science*, *9*(1), 283–310. <https://doi.org/10.1146/annurev-marine-122414-034032>
- Trimborn, S., Thoms, S., Petrou, K., Kranz, S. A., & Rost, B. (2014). Photophysiological responses of Southern Ocean phytoplankton to changes in CO₂ concentrations: Short-term versus acclimation effects. *Journal of Experimental Marine Biology and Ecology*, *451*, 44–54. <https://doi.org/10.1016/j.jembe.2013.11.001>
- Tsuji, Y., & Yoshida, M. (2017). Biology of haptophytes: Complicated cellular processes driving the global carbon cycle. *Advances in Botanical Research*, *84*, 219–261. <https://doi.org/10.1016/bs.abr.2017.07.002>
- Tyrrell, T., & Merico, A. (2004). *Emiliana huxleyi*: Bloom observations and the conditions that induce them. In *Coccolithophores* (pp. 75–97). Springer. https://doi.org/10.1007/978-3-662-06278-4_4
- von Dassow, P., Ogata, H., Probert, I., Wincker, P., Da Silva, C., Audic, S., et al. (2009). Transcriptome analysis of functional differentiation between haploid and diploid cells of *Emiliana huxleyi*, a globally significant photosynthetic calcifying cell. *Genome Biology*, *10*(10), R114. <https://doi.org/10.1186/gb-2009-10-10-r114>
- Waldbusser, G. G., Hales, B., Langdon, C. J., Haley, B. A., Schrader, P., Brunner, E. L., et al. (2015). Saturation-state sensitivity of marine bivalve larvae to ocean acidification. *Nature Climate Change*, *5*(3), 273–280. <https://doi.org/10.1038/nclimate2479>
- Walker, C. E., Taylor, A. R., Langer, G., Durak, G. M., Heath, S., Probert, I., et al. (2018). The requirement for calcification differs between ecologically important coccolithophore species. *New Phytologist*, *220*(1), 147–162. <https://doi.org/10.1111/nph.15272>
- Xu, H., Liu, H., Chen, F., Zhang, X., Zhang, Z., Ma, J., et al. (2023). Ocean acidification affects physiology of coccolithophore *Emiliana huxleyi* and weakens its mechanical resistance to copepods. *Marine Environmental Research*, *192*, 106232. <https://doi.org/10.1016/j.marenvres.2023.106232>
- Zeebe, R. E., & Wolf-Gladrow, D. (2001). *CO₂ in seawater: Equilibrium, kinetics, isotopes* (Vol. 65). Gulf Professional Publishing.
- Zhang, Y., & Gao, K. (2021). Photosynthesis and calcification of the coccolithophore *Emiliana huxleyi* are more sensitive to changed levels of light and CO₂ under nutrient limitation. *Journal of Photochemistry and Photobiology B: Biology*, *217*(January), 112145. <https://doi.org/10.1016/j.jphotobiol.2021.112145>
- Ziveri, P., de Bernardi, B., Baumann, K.-H., Stoll, H. M., & Mortyn, P. G. (2007). Sinking of coccolith carbonate and potential contribution to organic carbon ballasting in the deep ocean. *Deep Sea Research Part II: Topical Studies in Oceanography*, *54*(5–7), 659–675. <https://doi.org/10.1016/j.dsr2.2007.01.006>
- Zondervan, I., Zeebe, R. E., Rost, B., & Riebesell, U. (2001). Decreasing marine biogenic calcification: A negative feedback on rising atmospheric pCO₂. *Global Biogeochemical Cycles*, *15*(2), 507–516. <https://doi.org/10.1029/2000GB001321>